Geomorphology 456 (2024) 109211

Contents lists available at ScienceDirect

Geomorphology

journal homepage: www.journals.elsevier.com/geomorphology

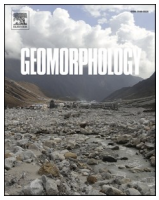

Sediment resuspension and transport due to synoptic winter winds in the Bohai Sea

Aimei Wang [a,b], David K. Ralston [c], Naishuang Bi [a,b], Xiao Wu [a,b], Chenghao Wang [d], Ping Yuan [e], Houjie Wang [a,b,*]

[a] College of Marine Geosciences, Key Laboratory of Submarine Geosciences and Prospecting Techniques, Ocean University of China, 238 Songling Rd., Qingdao 266100, China
[b] Laboratory of Marine Geology, Qingdao National Laboratory of Marine Science and Technology, Qingdao 266237, China
[c] Applied Ocean Physics and Engineering Department, Woods Hole Oceanographic Institution, Woods Hole, MA 02543, USA
[d] National Engineering Research Center of Port Hydraulic Construction Technology, Tianjin Research Institute for Water Transport Engineering, M.O.T., Tianjin 300456, China
[e] Department of Marine Environmental Engineering Technology, National Marine Environmental Monitoring Center, Dalian 116023, China

ARTICLE INFO

Keywords:
Storms
Current
Sediment dynamics
Suspended sediment concentration (SSC)
Bohai Sea

ABSTRACT

The Bohai Sea is the receiving basin of the Yellow River (Huanghe), one of the largest contributors of global terrestrial materials to the sea. An area of fine-grained sediment deposition extends northeast of the Yellow River and its formation mechanism is still unclear. A calibrated, high-resolution coupled model of the Bohai and Yellow Seas was used to investigate sediment transport pathways in the region under the influence of strong and varying winds in winter. Numerical results highlight the importance of storm events in modifying the regional sediment resuspension and transport. During winter, the prevailing winds are typically from the northeast and northwest, interspersed by relaxation periods with weak winds. Winds influenced the currents and sediment movement in the Bohai Sea through several processes: local wind waves and resuspension, coastal-trapped waves in the Bohai Sea, and remotely forced coastal-trapped waves in the Yellow Sea. During northwesterly winds, sediment off the Yellow River Delta was mainly transported eastward along the south coast of Bohai Sea and escaped the Bohai Sea through the southern Bohai Strait. When northeasterly winds prevailed, sediment transport split into three branches: westward into the Bohai Bay, northeastward to the central Bohai Sea, and eastward along the south coast of Bohai Sea. Modeling results driven by synoptic winds indicate a more complex sediment transport pattern than previously understood with monthly average wind forcing. These findings challenge the traditional view of predominantly eastward sediment transport during winter and help to explain the observed grain size distribution in the Bohai Sea, in particular the accumulation of fine-grained sediments northeast of the Yellow River.

1. Introduction

Meteorological events such as storms can profoundly impact sediment redistribution on continental shelves (Qin et al., 1986, 1989; Sanford, 1994; Shi et al., 2008; Brand et al., 2010; Bian et al., 2013; Zeng et al., 2015; Fan et al., 2019). As waves develop from wind input, wave-orbital motions apply stress to the seabed, which along with current-induced stress, can lead to local sediment resuspension (Grant and Madsen, 1979; Sanford, 1994; Warner et al., 2008; Miles et al., 2013; Fan et al., 2019). Strong winds further enhance wind-driven circulation (Li et al., 2015) and modify the length scales and direction of sediment transport (Brand et al., 2010; Yang et al., 2011; Zeng et al., 2015). The intensity, direction, and duration of the wind play crucial roles in determining the patterns of circulation and sediment transport (Enriquez, 2004; Paduan et al., 2018; Shen et al., 2019; Wang et al., 2021; Hsu, 2022). Given the importance of sediment dynamics for coastal morphology, marine biogeochemical cycling, and benthic ecosystems, investigating the impacts of varying wind conditions on sediment transport and deposition are essential for understanding global material cycling (Schoellhamer, 1995; Brand et al., 2010; Dong et al., 2011).

The Bohai Sea is the receiving basin for several rivers, including the Yellow River (Huanghe), the Haihe River, the Luanhe River, and the

* Corresponding author at: College of Marine Geosciences, Ocean University of China, 238 Songling Road, Qingdao 266100, China.
E-mail address: hjwang@mail.ouc.edu.cn (H. Wang).

https://doi.org/10.1016/j.geomorph.2024.109211
Received 4 August 2023; Received in revised form 12 April 2024; Accepted 12 April 2024
Available online 15 April 2024

Liaohe River (Fig. 1). The Yellow River has one of the highest sediment loads on Earth, discharging about 1.08 × 10^9 t of sediment per year (Milliman and Meade, 1983). Since a shift in the distributary network in 1855, the Yellow River has re-entered the Bohai Sea and been its dominant source of sediment. Due to seasonal variations in river discharge, the subaqueous Yellow River Delta acts as a sediment sink in summer and a source of sediment for redistribution in the Bohai Sea in winter (Wang et al., 2014). >60 % of the annual water and sediment discharge occurs during the summer and early fall (July–October) (Wang et al., 2007), particularly during the Water and Sediment Regulation Scheme that has artificially regulated the regime of water and sediment discharge since 2002.

In the summer, river-delivered sediment typically deposits around the Yellow River mouth due to the weak winds of the summer monsoon, tidal shear fronts, and strong stratification (Bi et al., 2010). Additionally, sediment can be transported along the west side of the central Bohai Basin by weak southeasterly winds in summer (Wang et al., 2008; Cheng et al., 2021). In contrast, during the winter (October–March), stronger northerly monsoon winds lead to active sediment resuspension by large waves and transport into the Bohai Basin and the Yellow Sea (Bi et al., 2011; Yang et al., 2011). Based on hydrographic surveys, satellite images, and modeling results, a long-held consensus is that strong northerly winds in winter transport sediment eastward from the Yellow River Delta along the south coast of Bohai Sea and into the Yellow Sea through the southern Bohai Strait (Jiang et al., 2000; Bi et al., 2011; Lu et al., 2011; Bian et al., 2013; Liu et al., 2020). However, grain-size analyses of surface sediments suggest inconsistencies with this long-held consensus (Qiao et al., 2010; Yuan et al., 2020). Fine-grained sediment covers the central and southern Bohai Sea, extending northeastward from the Yellow River into the western Liaodong Bay (Fig. 1, Marine Geology Laboratory of Institute of Oceanology Chinese Academy of Sciences, 1985; Qiao et al., 2010; Yuan et al., 2020). Transport patterns inferred using the Gao-Collins grain size trend analysis method indicated that sediment was primarily transported northeastward from the Yellow River mouth, contrary to the eastward direction towards the Yellow Sea. Discrepancies between the methodologies might be attributed to the limited temporal and spatial coverage of measurements (Bi et al., 2011; Yang et al., 2011) and models driven by monthly or seasonally averaged meteorological forcing (Jiang et al., 2000; Lu et al., 2011; Bian et al., 2013; Liu et al., 2020).

Currents and sediment resuspension in the Bohai Sea are sensitive to seasonal monsoon forcing (Bian et al., 2013; Wang et al., 2014). In summer, currents flow northeastward into the central Bohai Sea, driven by weak southeasterly winds and thermal stratification. In contrast, the winter circulation driven by powerful northerly winds features an eastward outflow via the southern Bohai Strait and a westward inflow through the northern part of the strait (e.g., Wang et al., 2008; Lu et al., 2011; Zhou et al., 2017). However, the prevailing winds in winter are occasionally interrupted by periods of relaxation, and this significantly affects circulation and sediment transport patterns (Yuan et al., 2008; Wan et al., 2015; Hu et al., 2017; Ding et al., 2018, 2019; Wu et al., 2019a, 2019b; Wang et al., 2020). For example, during brief relaxations in strong northeasterly winds, a counter-wind current developed in the western Taiwan Strait (Shen et al., 2019). In the southwestern Taiwan Strait, three distinct current patterns were identified influenced by varying wind conditions: downwind currents during strong winds, upwind currents in low wind conditions, and a gradual transition of current patterns in medium wind conditions (Wang et al., 2021). Hsu (2022) observed a southward flow during intense northeastern monsoons and a northward current under weaker northerly or even southerly winds in the Penghu Channel. In the Bohai Strait, strongly southward currents are intensified by northerly winds, whereas strongly northward currents follow when the wind weakens or shifts (Wan et al., 2015; Duan et al., 2020). Similarly, Wu et al. (2019a) reported a net sediment influx into the Bohai Sea after a northerly wind event during a winter cruise, challenging the traditional view of sediment transport out of the basin through the Bohai Strait in winter. Furthermore, based on an 11-day mooring observation, Duan et al. (2020) estimated that about 25 % of the total sediment transport from the Bohai Sea to the Yellow Sea during a strong northerly wind event returned to the Bohai Sea through the Bohai Strait during the subsequent wind relaxation periods.

In addition to temporal variability, modest shifts in wind direction can have important impacts on coastal currents and sediment transport. For example, a 10-degree shift in wind direction in Monterey Bay was found to create two different gyres with opposite circulations (Enriquez, 2004). Previous studies of the Bohai Sea have primarily categorized the prevailing winter winds as uniformly northerly, without differentiating between northeasterly and northwesterly variations (Ding et al., 2018; Wu et al., 2019a; Wang et al., 2020). However, both northwesterly and northeasterly winds occur prominently in winter, and wind direction may influence anomalies in water levels, currents, and sediment transport in this shallow, semi-enclosed region.

In this study, a calibrated model, driven by realistic 6-hourly surface winds from a reanalysis product was used to simulate the patterns of current and sediment transport in the Bohai Sea under typical winter storm conditions, including variability in direction (northeasterly and northwesterly) and unsteadiness (strengthening, ceasing, and turning). The processes contributing to the sediment deposition patterns in the

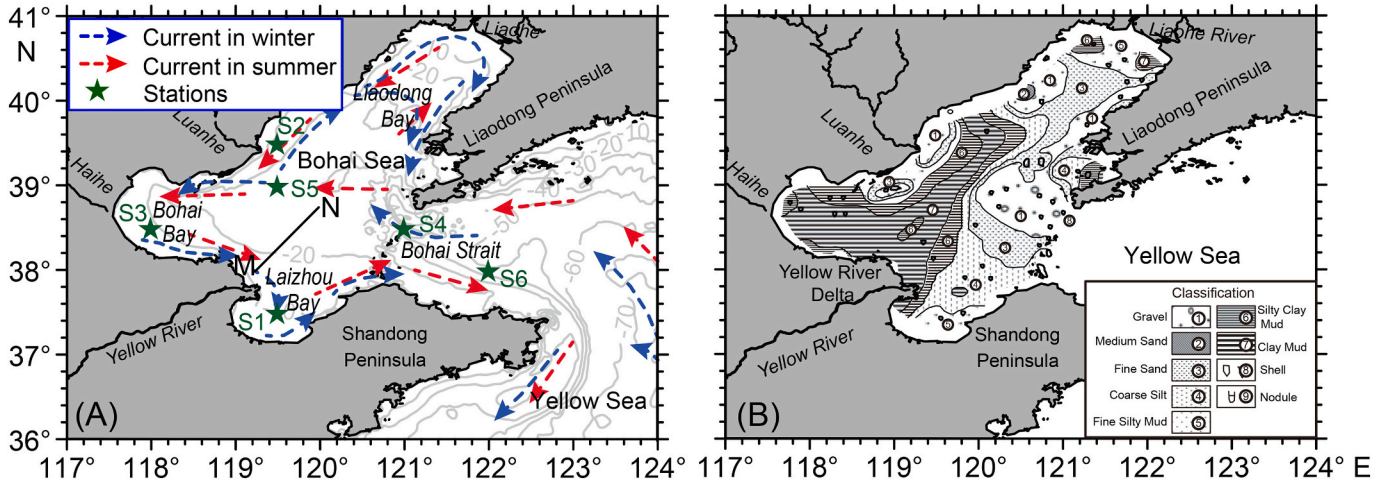

Fig. 1. Study area (A), general pattern of seasonal circulation systems in the Bohai Sea (modified after Guan, 1994; Fang et al., 2000) and classification of surface sediment in the Bohai Sea (B, modified from Marine Geology Laboratory of Institute of Oceanology Chinese Academy of Sciences (1985)).

model were diagnosed through idealized model experiments (Table 1) designed to identify the effects of specific forcing factors. Model results are synthesized and used to help interpret the observed sediment grain size patterns that in part motivated this study.

2. Regional setting

The Bohai Sea, located in northeastern China, is a shallow, semi-enclosed inner shelf sea surrounded by the mainland and the Liaodong Peninsula. It contains three main bays (e.g., Laizhou Bay, Bohai Bay, and Liaodong Bay) and the central Bohai Basin. The Bohai Sea connects to the Yellow Sea through the narrow Bohai Strait to the east (Fig. 1). The average depth of the Bohai Sea is about 18 m, with the deepest part (~ 70 m) situated in the northern part of the Bohai Strait (Qin and Li, 1983).

Terrestrial sediment from several rivers, particularly the Yellow River, which delivers about 1.08 $\times 10^9$ t of sediment per year (Milliman and Meade, 1983), leads to the formation of several muddy depositional areas in the Bohai Sea. Fine-grained sediment (fine silt, silty clay, and clay) with a median size of 4–8 Φ covers most of the southwestern Bohai Sea, extending northeastward from the Yellow River Delta to the central Bohai Basin. The surface sediment in the eastern Bohai Sea is coarser, mainly consisting of fine sand and coarse silt (Marine Geology Laboratory of Institute of Oceanology Chinese Academy of Sciences, 1985).

Tides in the Bohai Sea are mixed semidiurnal type with two counter-clockwise semi-diurnal amphidromic systems (M_2 and S_2) (Sun and Xi, 1988). Mean tidal currents at the mouth of Laizhou Bay are about 20 cm s^{-1}, increasing to 80 cm s^{-1} in the northern Bohai Strait and the eastern part of Liaodong Bay (Huang et al., 1999). Residual currents induced by the tides are generally weak, with mean velocities <5 cm s^{-1}, except for a pair of cyclonic and anticyclonic headland eddies in the Bohai Strait (Huang et al., 1999).

The climate of the Bohai Sea exhibits distinct seasonal variability, closely associated with monsoon activity. During the winter (October to March), strong winds, primarily from the northwest and northeast, reach maximum speeds of >11 m s^{-1} (Yang et al., 2011). Conversely, summer is characterized by weak southerly winds. These seasonally varying atmospheric conditions, coupled with freshwater influx, significantly influence the circulation patterns of the Bohai Sea. During the winter, the mean circulation flows into the Bohai Sea through the northern part of the Bohai Strait and separates into two branches (Fig. 1). One branch flows northward along the west coast of Liaodong Bay, while the other flows into Bohai Bay, turns southward along its west coast, then turns eastward along the Yellow River Delta and Laizhou Bay, eventually exiting through the southern part of the Bohai Strait (Guan, 1994; Fang et al., 2000). Summer sees the formation of a cyclonic current within the Liaodong Gyre (Guan, 1994) driven by the predominantly southerly winds, marking a reversal from the winter circulation pattern.

Due to the shallow nature of the Bohai Sea, suspended sediment concentration (SSC) and sediment transport also exhibit strong seasonal variability through the influence of the monsoon on wind waves and coastal currents. Studies have consistently found greater SSC and sediment flux in winter compared to summer, including along the Yellow River Delta, near the mouth of Bohai Bay, and west of the headland of Liaodong Peninsula (Bi et al., 2011; Yang et al., 2011; Wang et al., 2014). Almost 70 % of the sediment input from the Yellow River deposits within 15 km of its mouth (Qin and Li, 1983). A portion of this sediment is transported eastward to the open ocean through the southern Bohai Strait (Qin and Li, 1983; Martin et al., 1993; Bi et al., 2011), becoming a primary source of mud deposits in the Yellow Sea (e.g., the mud wedge or distal subaqueous delta off the eastern Shandong Peninsula) (Alexander et al., 1991; Cheng et al., 2004; Liu et al., 2004; Yang and Liu, 2007; Bi et al., 2011; Wang et al., 2019) and to the south of Cheju Island, off the southern coast of South Korea (Milliman and Meade, 1983).

Table 1
Settings of numerical experiments.

	Control run	Experiment 1	Experiment 2	Experiment 3
Tides	√	√	×	×
Winds	√	×	√	√*

1 * u component of wind direction was reversed but the velocity magnitude in Experiment 3 was the same to that of control run.
2 Symbols √ and × denote the experiments with and without the corresponding forces, respectively.

3. Methods

The Coupled Ocean-Atmosphere-Wave-Sediment Transport (COAWST, Warner et al., 2008, 2010) Modeling System was utilized in this study. This system integrates several state-of-the-art modeling components: the Regional Ocean Modeling System (ROMS, Shchepetkin and Mcwilliams, 2005) for ocean circulation, the Simulating Waves Nearshore (SWAN, Booij et al., 1999) for waves, and the Community Sediment Transport Modeling System (CSTMS, Warner et al., 2008) for sediment transport. These models are coupled through the Modeling Coupling Toolkit (MCT, Jacob et al., 2005; Larson et al., 2005). ROMS and SWAN are two-way coupled, with SWAN providing wave information to ROMS including spectral wave heights, wavelengths, average wave periods at the surface and near the bottom, wave propagation direction, near-bottom orbital velocity, and wave energy dissipation rate. ROMS supplies SWAN with water depth, sea-surface elevation, and current velocity. The modeling domain covers the Bohai, Yellow and East China Seas to minimize the influence of open boundary conditions. The grid resolution is 1.5′ in the horizontal and there are 30 uniform layers in the vertical dimension. To calculate the bottom shear stress, the wave-current Bottom Boundary Layer (BBL) model (ssw_bbl) developed by Madsen (1994) is implemented (Warner et al., 2008).

The SWAN model uses the same horizontal grid and bathymetry as ROMS. It is driven by wind from the European Centre for Medium-Range Weather Forecasts (ECMWF) reanalysis model (ERA-Interim). At the open ocean boundary, the peak wave period, average wave direction at the peak period, and significant wave heights are interpolated from the Wave-Watch III model products (http://polar.ncep.noaa.gov/waves/index2.shtml). Coupled model variables are exchanged between SWAN and ROMS every hour.

In the sediment module, three particle classes are defined: clay, silt, and sand. The initial condition for seabed composition incorporates four characteristic bottom types, each consisting of different proportions of the particle classes (sand, clayey silty sand, clayey silt, silty clay). The settling velocity for these particles (clay: 0.5 mm s^{-1}; silt: 1.0 mm s^{-1}; sand: 15.3 mm s^{-1}) is adopted following Wang et al. (2020). Further details on the model set-up can be found in Wang et al. (2019). The model performance was evaluated against observations of tides, water levels, currents, waves, temperature, and SSC in previous studies (Wang et al., 2019, 2022). To focus on sediment transport by wind events in winter, the simulations presented here were run from October 1, 2006 to January 1, 2007, covering a period of field observations off the Yellow River Delta. To assess the effect of wind direction on variations in current and sediment flux, four numerical experiments were conducted (Table 1). The control run included all driving forces (winds and tides). Experiment 1 used only the tides and no wind to focus on the influence of tides on the currents and sediment transports. Alternatively, in Experiment 2, tides were eliminated, and only winds were considered. To explore the effect of wind direction on currents and sediment fluxes, Experiment 3 was similar to Experiment 2 but with the east-west component of the wind reversed compared to the control run. Currents calculated from models were filtered using Godin-type filters, which are effective in removing diurnal, semidiurnal, and shorter period fluctuations from the hourly model output (Thomson and Emery, 2014).

Observational datasets were obtained from cruises of R/V

DONGFANGHONG 2 (offshore observations) and two smaller ships (nearshore observations) in the Bohai Sea after winter storms during the period November 7–14, 2006. Water samples for SSC measurements were collected at six different depths, with bottom water samples taken from 2 to 3 m above the seabed. Further details on water sampling and data collection can be found in Yang et al. (2011).

4. Results

4.1. Suspended sediment variation based on observations and models

To compare the model results with observational data, averaged SSC from the model and measurements from November 7–14, 2006 are presented in Fig. 2. Both modeled and observed results showed that the SSC in the Bohai Sea was generally high with strong vertical mixing (Fig. 2A, B, C, and D). The highest SSC, with values >100 mg L^{-1}, were observed along the Yellow River Delta, at the mouth of Bohai Bay, and at the head of Liaodong Bay, with concentrations diminishing seaward. In contrast, the SSC in the central Bohai Basin was generally low, with values <30 mg L^{-1}. After strong northwesterly winds (Fig. 3A), currents flowed eastward from the Bohai Sea into the Yellow Sea through the southern Bohai Strait (Fig. 2E). In the northern part of the Bohai Strait, currents entered the Bohai Sea, leading to the formation of an anticyclonic gyre in the central Bohai Basin (Fig. 2E). The dominant sediment transport was from the Yellow Sea into the Bohai Sea, where it divided into two branches towards Liaodong Bay and Bohai Bay. Eastward sediment transport along the southern coast of the Bohai Sea and into the Yellow Sea through the southern Bohai Strait was much weaker (Fig. 2F).

Strong wind events from the northeast and northwest generally persist for 2–3 days, and are interspersed with periods of weaker winds (Fig. 3A). In November 2006, four strong storm events were identified, characterized by large values of SSC. These large SSC values were mainly due to local wave-induced resuspension in the shallow waters (Fig. 3). Mean water levels and the direction of residual currents showed sensitivity to wind direction (Fig. 3B). Under northwesterly winds (events I and II), a decrease in water level was observed off the Yellow River Delta, and water levels returned to fair-weather conditions once the winds subsided. Conversely, during northeasterly winds (events III and IV), increases in mean water levels were recorded. The currents flowed

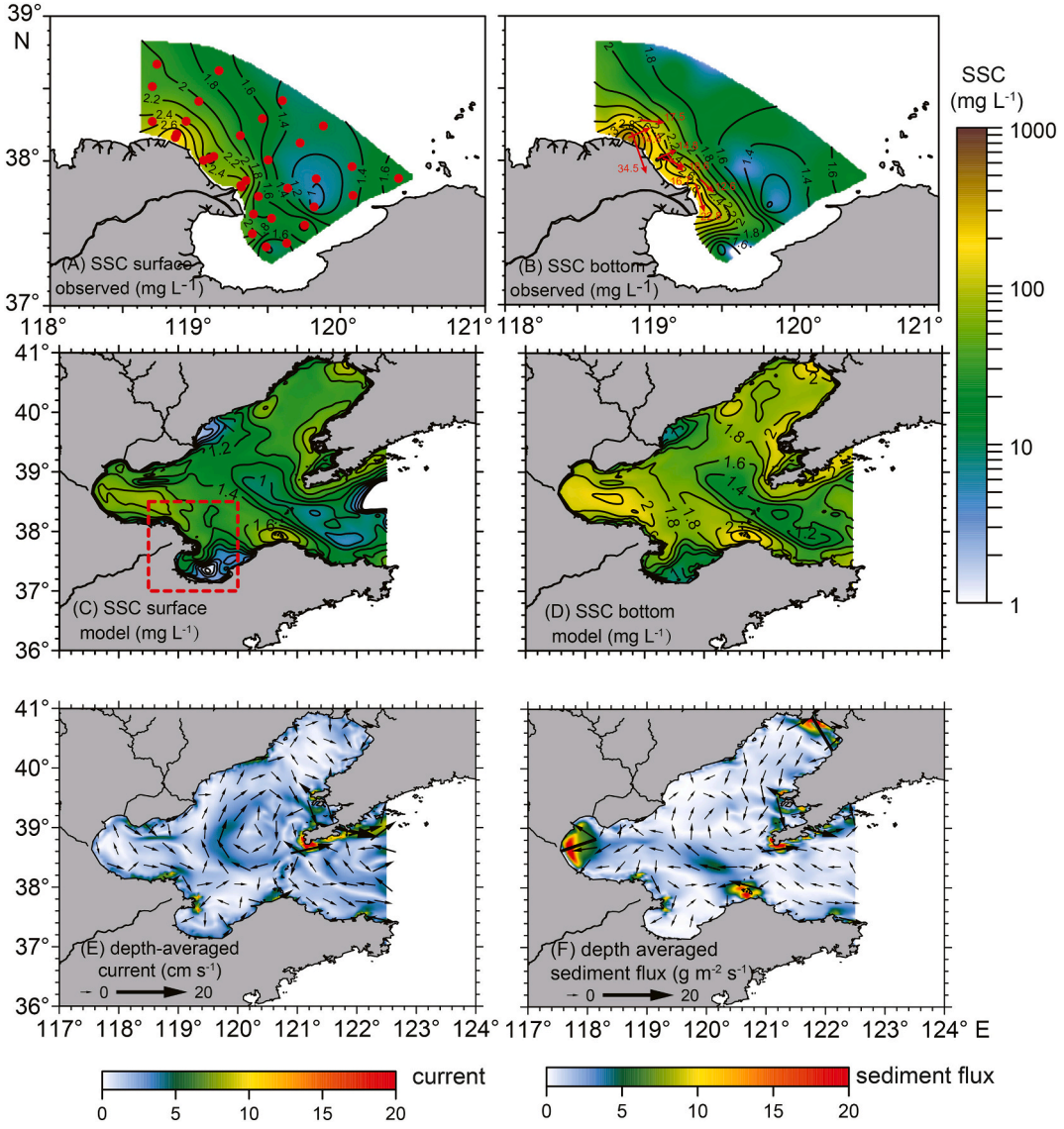

Fig. 2. Horizontal distributions of SSC from observation and modeled results in the Bohai Sea on November 7–14: observed surface (A) and bottom (B) SSC, modeled surface (C) and bottom (D) SSC, and modeled depth-averaged currents (E) and sediment flux (F). Red points in Fig. 2A were survey stations in November 2006, Red arrows in Fig. 2B were observed depth-averaged residual current.

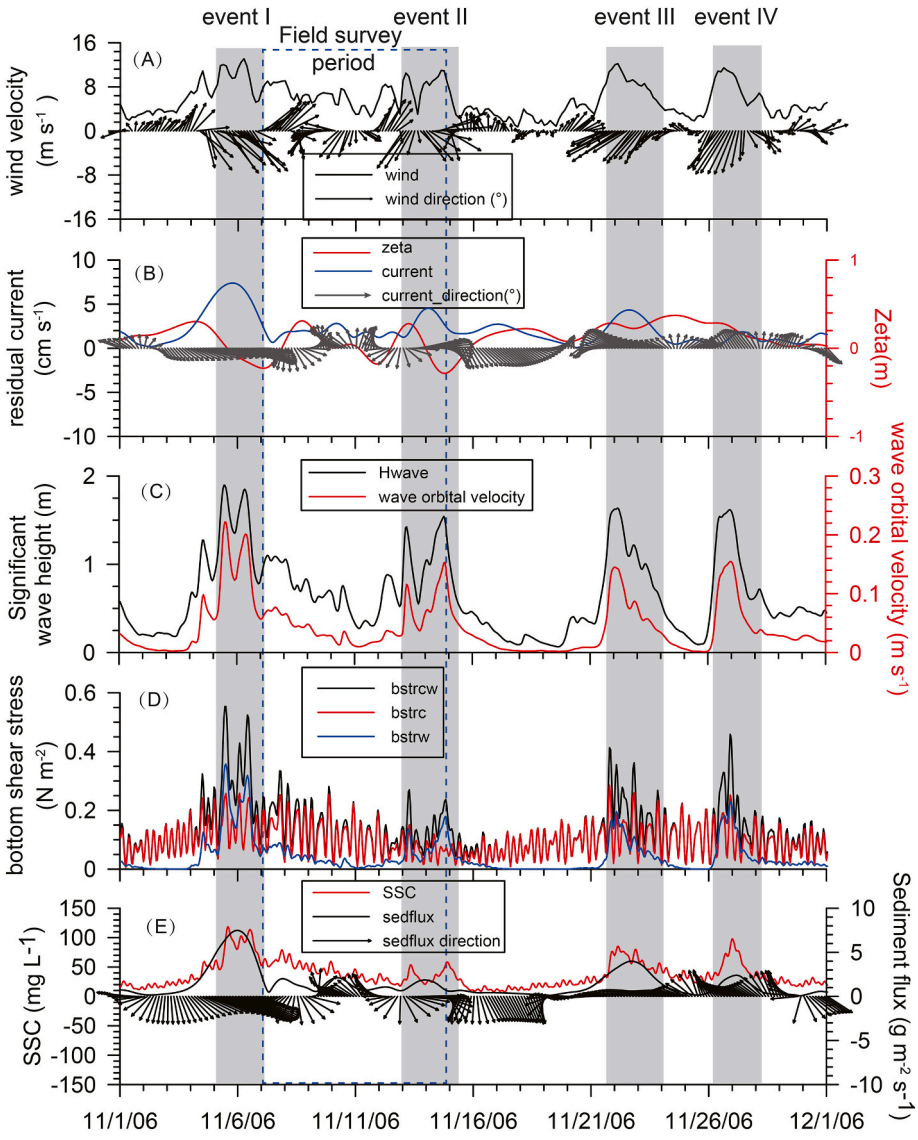

Fig. 3. Spatially averaged (A) wind speed and wind vectors at 10 m above the sea surface, (B) water level and depth-averaged residual current, (C) significant wave height and wave orbital velocity, (D) bottom shear stress, and (E) depth-averaged SSC and sediment flux from modeled results in the southern Bohai Sea in 2006. The domain for spatial average is shown in Fig. 2 (C) as the red dashed line.

in the direction of the wind stress during northwesterly winds (Fig. 3B events I and II), whereas during northeasterly winds, currents off the Yellow River Delta flowed northwestward, deviated from the wind direction (Fig. 3B events III and IV). The instantaneous depth-averaged sediment flux typically aligned with the current direction, moving southeastward with northwesterly winds and northwestward with northeasterly winds. However, the magnitude of the sediment flux varied with the variation of SSC, highlighting a significant influence of storm-induced resuspension (Fig. 3E).

4.2. *Spatial and temporal variations of currents in different stage of storm*

Given that the instantaneous depth-averaged sediment flux generally aligns with the direction of currents (Fig. 3), a comprehensive analysis was initially conducted on the spatial and temporal variations in water levels and currents during two storms characterized by northwesterly (event I, 5 to 6 Nov.) and northeasterly (event IV, 26 to 27 Nov.) winds. With the onset of northwesterly winds, currents in Liaodong Bay and the central Bohai Basin flowed southward, whereas along the south coast of the Bohai Sea, currents moved eastward, influenced by the coastal topographic constraint (Fig. 4A–H). The strong northwesterly winds facilitated water expulsion from the Bohai Sea through the entire Bohai Strait, leading to water level reduction in both Bohai and Liaodong Bays and a slight elevation along the northern coast of the Shandong Peninsula. As the winds weakened, coastal-trapped waves, driven by the sea-level differential between the Bohai and Yellow Seas (Ding et al., 2018; Wu et al., 2019a; Wang et al., 2020) flowed back into the Bohai Sea through the northern Bohai Strait, diverging into two branches. One branch flowed northward along the west coast of Liaodong Bay, and the other entered Bohai Bay along its north coast, later turning eastward along its south coast, thereby generating a cyclonic current in the central Bohai Bay. These currents continuously moved eastward along the Yellow River Delta and Laizhou Bay coasts, ultimately exiting the Bohai Sea through the southern Bohai Strait.

Current and water level variations under northeasterly winds differed markedly from those under northwesterly winds (Fig. 4I–P). With northeasterly winds, the sea level decreased in Liaodong Bay, whereas it rose along the southern coast of the Bohai Sea. This sea level disparity between the southern coast of the Bohai Sea and Liaodong Bay resulted in the division of currents near the Yellow River Delta into three

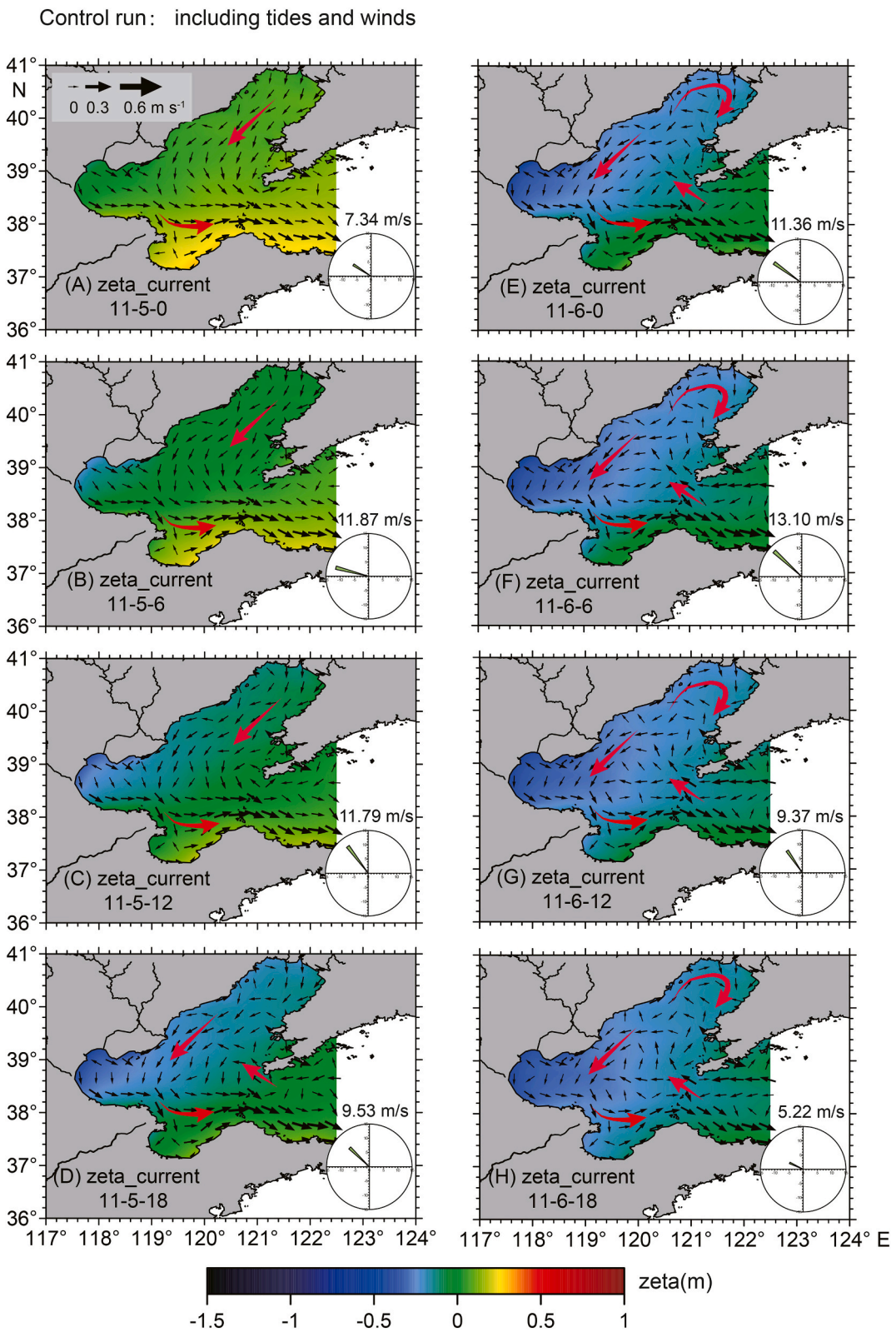

Fig. 4. Horizontal distribution of water level (color) and depth-averaged current (arrows) from the control modeled results on Nov. 5–6 and Nov. 26–27 and wind rose diagrams (lower right).

branches. A weak branch flowed westward into Bohai Bay along its south coast before turning eastward along its north coast. A second branch moved northeastward, forming an anti-cyclonic gyre in the central Bohai Sea, before exiting through the northern part of the Bohai Strait. A third branch flowed eastward along the south coast of the Bohai Sea, exiting through the southern Bohai Strait. Additionally, an anti-cyclonic gyre developed in the central Bohai Basin (Fig. 4I–L). Initially, as northeasterly winds set in, water was pushed out of the

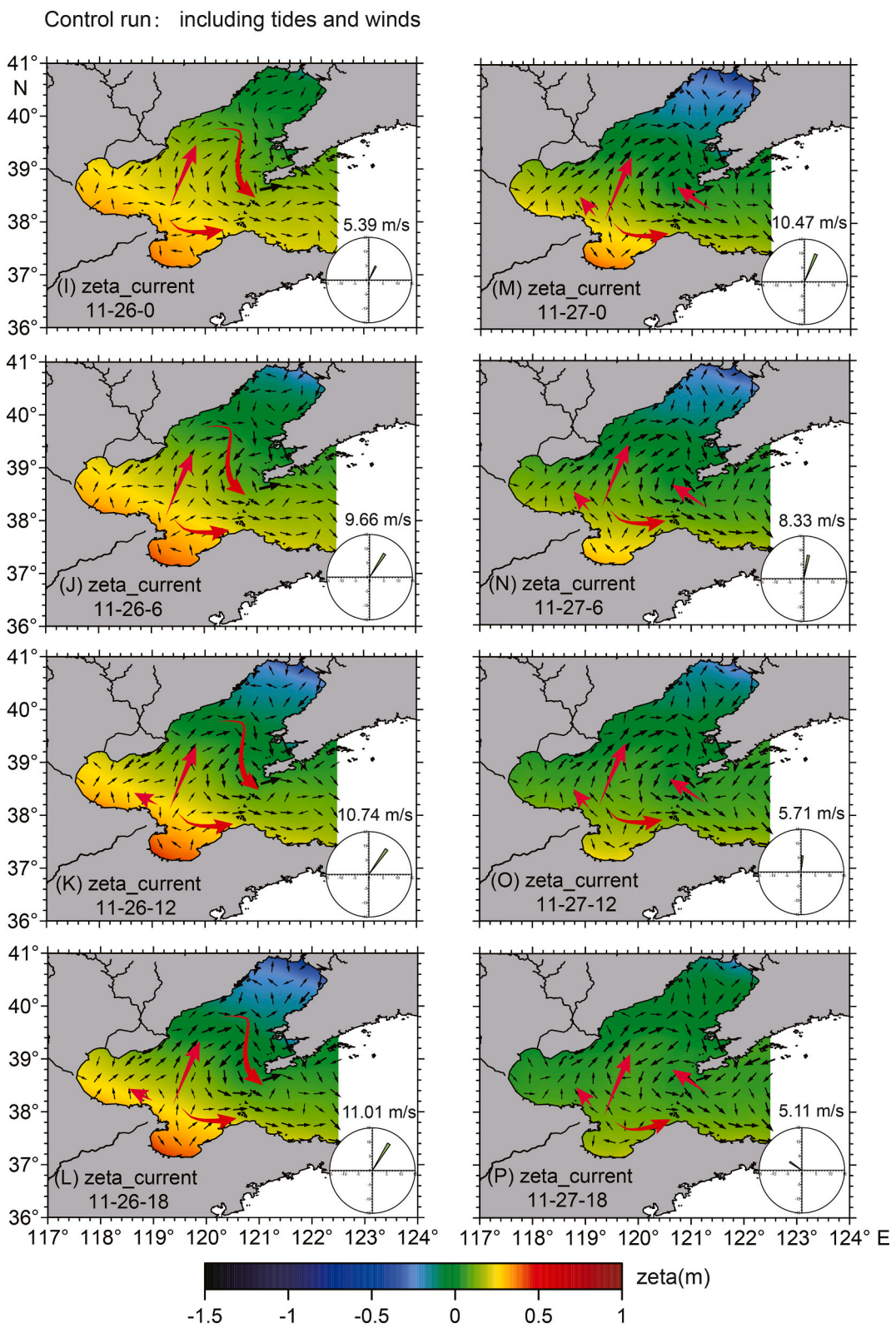

Fig. 4. (*continued*).

Bohai Sea through the entire Bohai Strait. However, as the winds weakened, the circulation pattern reversed, with water entering the Bohai Sea through the northern part of the Bohai Strait and exiting through the southern part (Fig. 4M–P).

4.3. Mechanism of currents variation

The circulation patterns in the Bohai Sea are significantly influenced by factors such as topography, hydrography, tides, wind stress, and sea level gradients (Teague and Jacobs, 2000; Yu et al., 2010; Yuan and Hsueh, 2010; Lin and Yang, 2011; Qu et al., 2018). Considering the

similarities in topographical and hydrographical conditions between events I and IV, these factors played a minimal role in differentiating the two events. To examine the contributions of tides and winds to the residual currents in the Bohai Sea, two experiments were conducted. Experiment 1, which isolated the effect of tides, resulted in weak currents flowing northeastward from the south coast of the Bohai Sea (Fig. 5), the formation of an anti-cyclonic gyre in the central Bohai Basin, and flow exiting through the entire Bohai Strait. The residual currents, when influenced by tides alone, showed similar patterns between events I and IV.

When tides were excluded in Experiment 2, currents and water levels showed similar patterns as the control run when northwesterly winds

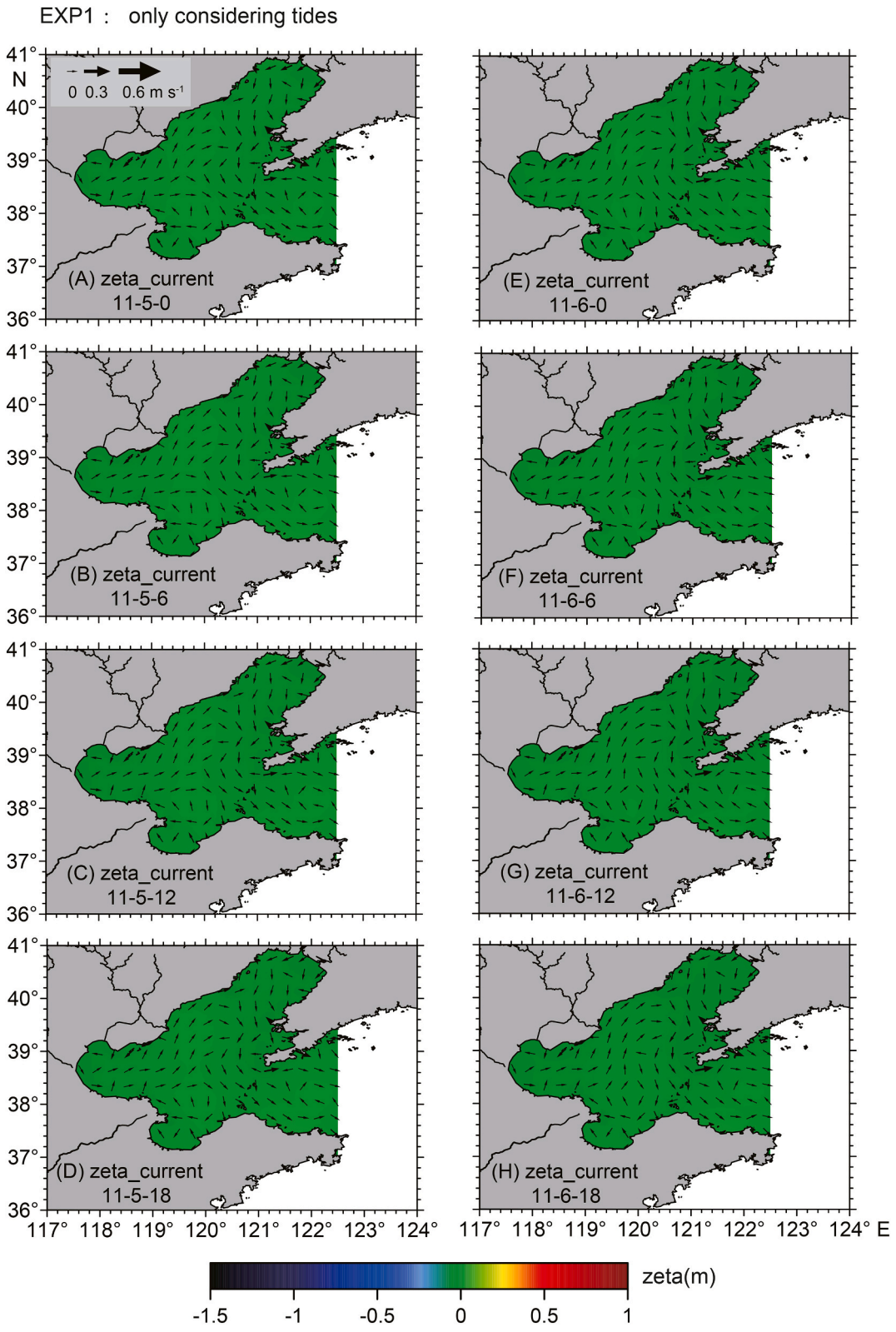

Fig. 5. Horizontal distribution of water level (color) and depth-averaged current (arrows) from Experiment 1 only considering tides on Nov. 5–6 and Nov. 26–27.

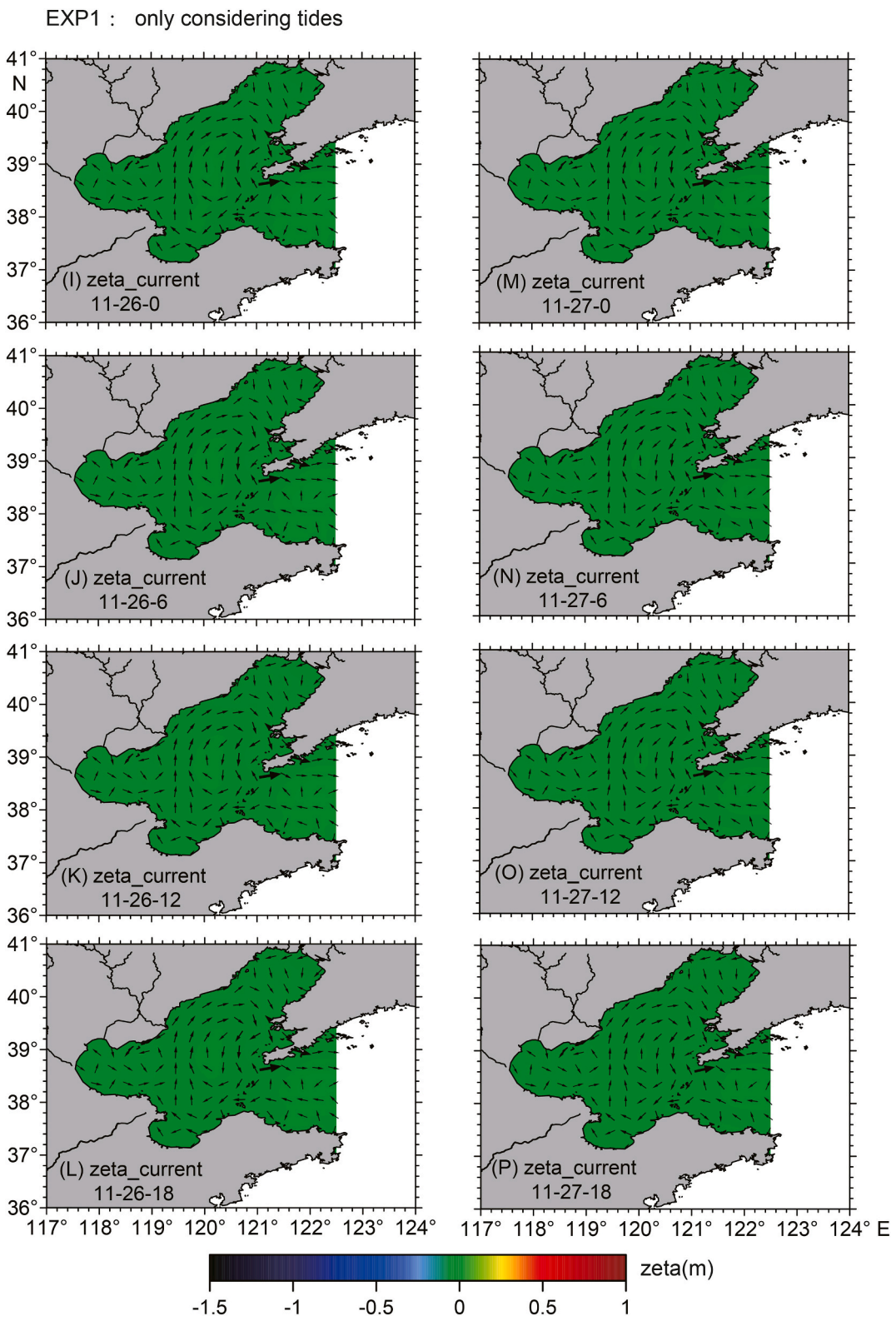

Fig. 5. (*continued*).

prevailed (Fig. 6), whereas the patterns were slightly different when northeasterly winds prevailed. During northwesterly winds, currents in Liaodong Bay flowed southwestward and turned eastward along the south coast of the Bohai Sea, eventually entering the Yellow Sea through the entire Bohai Strait. As the wind weakened, currents entered the Bohai Sea through the northern Bohai Strait and separated into two branches towards Liaodong Bay and Bohai Bay, with the current along the south coast of the Bohai Sea continuing eastward. Under northeasterly winds and without tidal influence, currents in the Bohai Sea increased and flowed southwestward in the direction of the wind stress before turning right in Bohai Bay (Fig. 6J), influenced by the Coriolis force, and splitting into three branches as in the control run. This

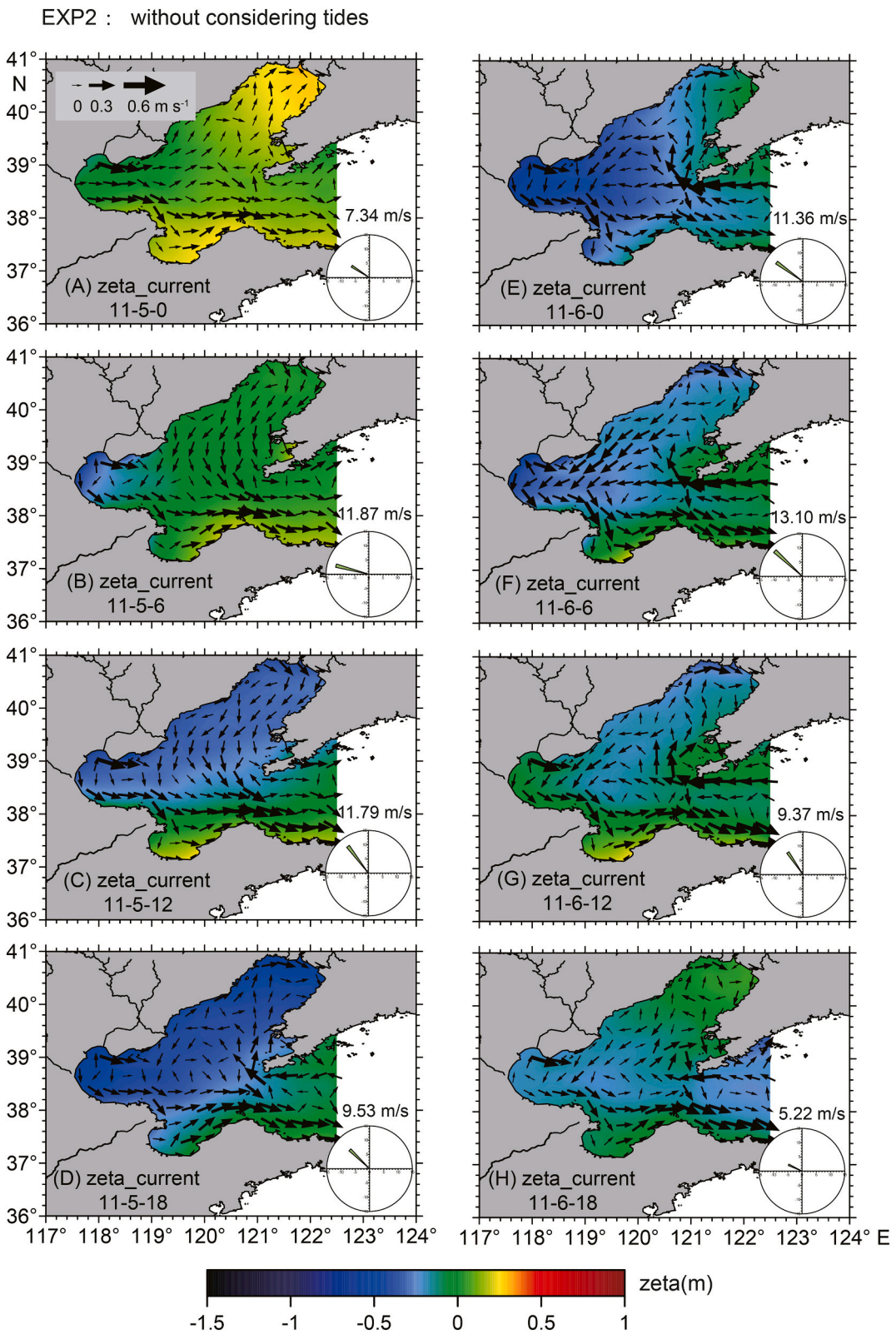

Fig. 6. Horizontal distribution of water level (color) and depth-averaged current (arrows) from Experiment 2 without tides on Nov. 5–6 and Nov. 26–27, with wind rose diagrams (lower right).

increase in velocity might be attributed to reduced effective bottom friction in the absence of tidal forces (Wu et al., 2018). The differences between the results of Experiment 2 and the control run indicated that local winds were an important force in changing regional circulation patterns.

Experiment 3 was designed to assess the influence of wind direction on residual current patterns by reversing the east-west wind direction while maintaining the same wind magnitude and excluding tidal forces.

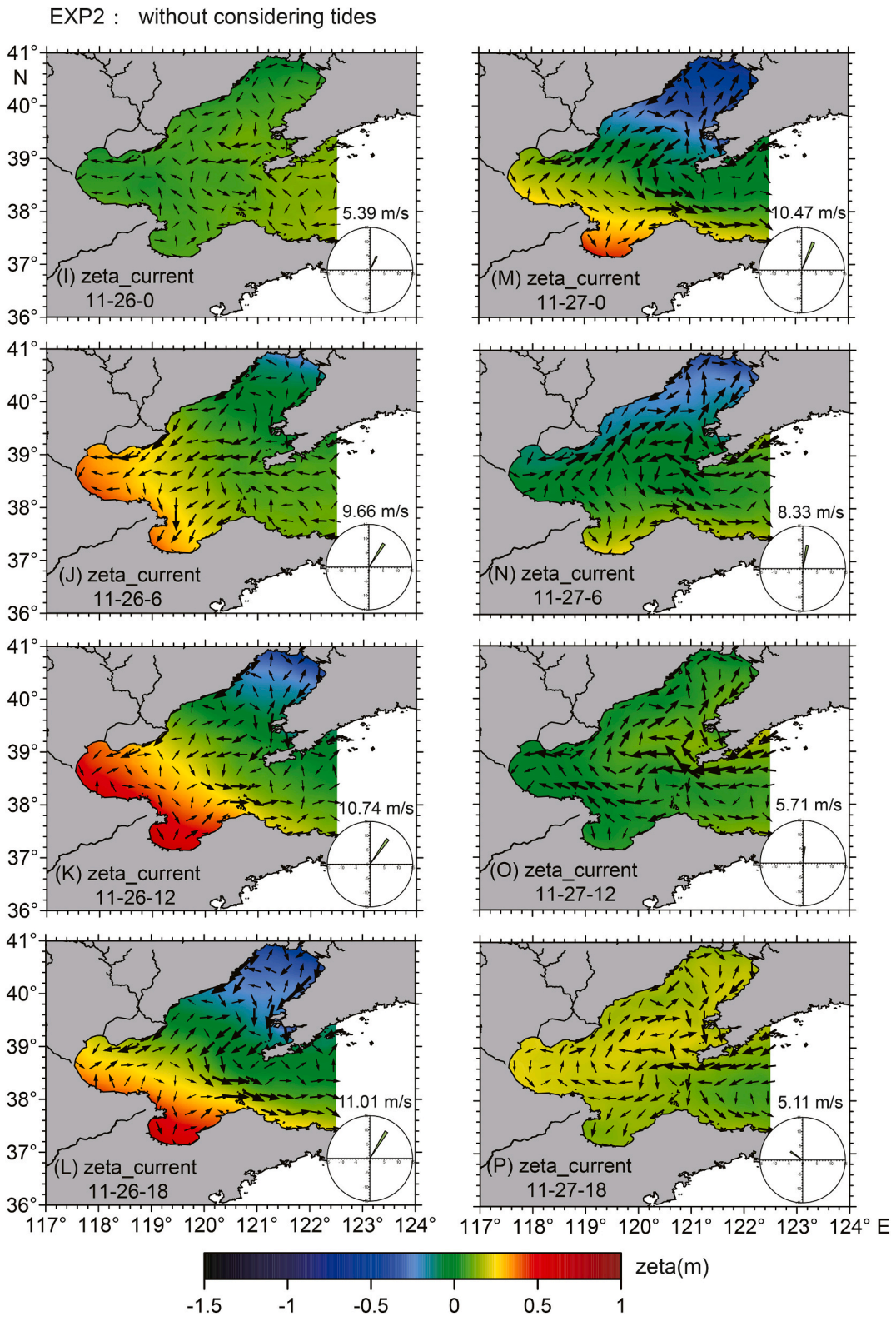

Fig. 6. (*continued*).

The model results demonstrated that residual current patterns were significantly influenced by the direction of the wind. Altering the wind direction led to noticeable changes in current and water level patterns compared to Experiment 2 (Figs. 6 and 7). Specifically, when the wind shifted from northwesterly to northeasterly, the patterns of current and water level aligned with those observed under the initial northeasterly wind conditions, including a rise in water level and the formation of three distinct branches of flow off the Yellow River Delta as the wind intensified (Figs. 6 and 7). Similarly, a change from northeasterly to northwesterly wind led to an eastward flow along the southern coast of the Bohai Sea, accompanied by a rapid decrease in water levels in both Liaodong Bay and Bohai Bay as the wind strength increased. Eastward

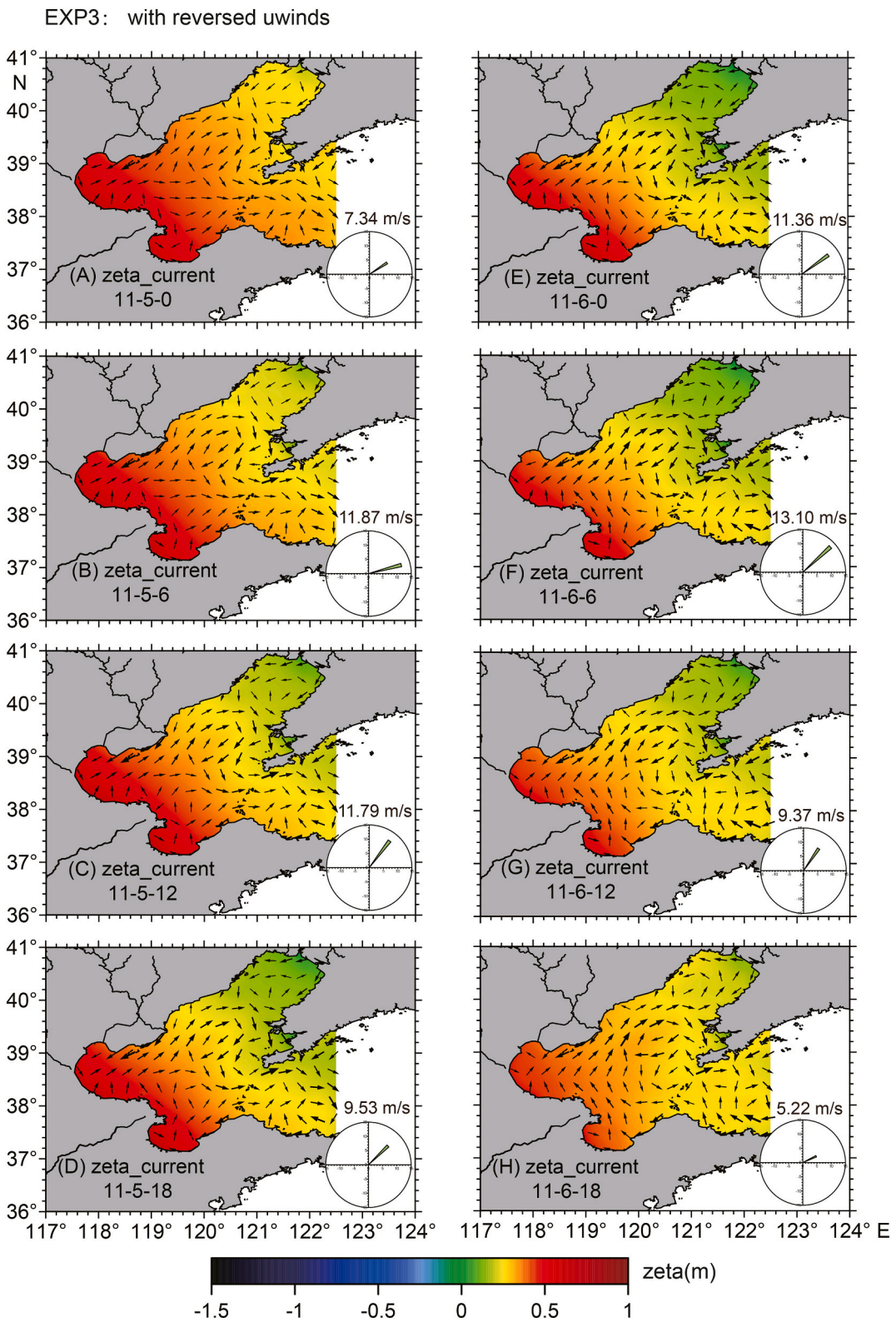

Fig. 7. Horizontal distribution of water level (color) and depth-averaged current (arrows) from Experiment 3 with reversed west-east wind components on Nov. 5–6 and Nov. 26–27, with wind rose diagrams (lower right).

currents exited the Bohai Sea via the southern Bohai Strait, while a westward current entered the Bohai Sea through the northern part, similar to the original northwesterly forcing conditions. These results underscore the crucial role of wind direction in modifying flow patterns and sediment transport pathways.

To examine the driving factors, the depth-averaged momentum terms were output from the model. The depth-averaged momentum terms equation in Cartesian coordinates follows the formulation pro-

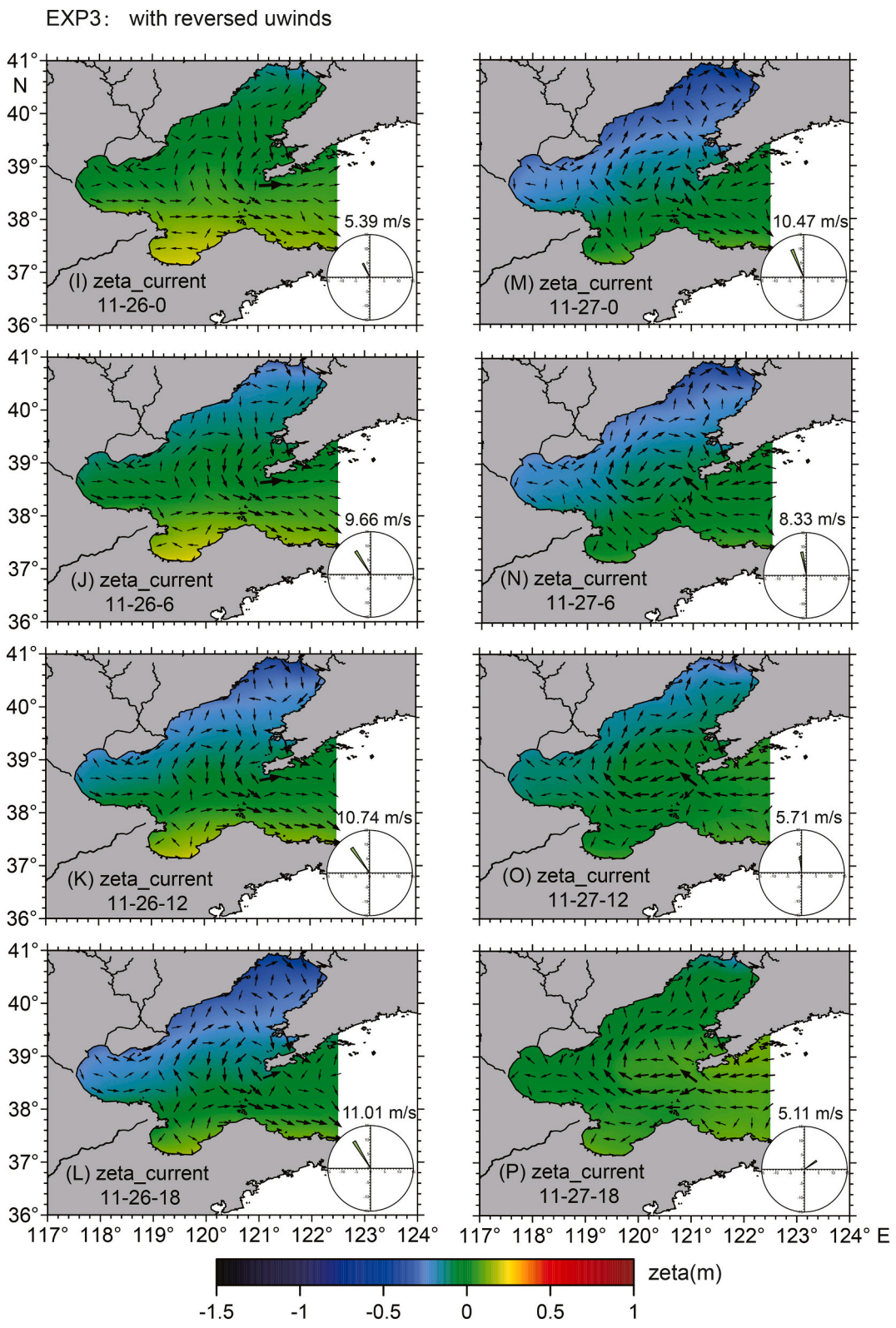

Fig. 7. (*continued*).

posed by Liu and Gan (2014):

$$\overbrace{\frac{\partial \overline{u}}{\partial t}}^{ACC_x} = \overbrace{f\overline{v}}^{COR_x} \overbrace{-[(\overline{u},\overline{v})\bullet\nabla]\overline{u}}^{HADV_x} \overbrace{-g\eta_x}^{PGF_x} + \overbrace{\frac{\tau_{sx}}{\rho_0 D}}^{SSTR_x} \overbrace{-\frac{\tau_{bx}}{\rho_0 D}}^{BSTR_x} + \overbrace{K_h\nabla^2\overline{u}}^{HVISC_x} \quad (1)$$

$$\overbrace{\frac{\partial \overline{v}}{\partial t}}^{ACC_y} = \overbrace{f\overline{u}}^{COR_y} \overbrace{-[(\overline{u},\overline{v})\bullet\nabla]\overline{v}}^{HADV_y} \overbrace{-g\eta_y}^{PGF_y} + \overbrace{\frac{\tau_{sy}}{\rho_0 D}}^{SSTR_y} \overbrace{-\frac{\tau_{by}}{\rho_0 D}}^{BSTR_y} + \overbrace{K_h\nabla^2\overline{v}}^{HVISC_y} \quad (2)$$

where subscripts x and y denote the zonal and meridional directions,

respectively. D represents the depth, and ρ_0 is the reference density. The variables τ_{sx}, τ_{sy}, τ_{bx}, and τ_{by} represent the surface and bottom stresses. The sea surface height (SSH) is denoted by η. The terms in Eqs. (1) and (2) include (1) acceleration (ACC), (2) Coriolis force (COR), (3) horizontal nonlinear advection (HADV), (4) pressure gradient force (PGF), (5) surface wind stress (SSTR), (6) frictional bottom stress (BSTR), and (7) horizontal viscous term (HVISC).

The variation in ocean currents is significantly influenced by a combination of surface wind stress, the pressure gradient, and the Coriolis force. To examine the spatial variability of momentum terms and water level variations across the zonal and meridional axes, as well as between the Bohai and Yellow Seas, six representative locations (S1–S6) were selected for analysis (Fig. 1A). Points S1 and S2 are positioned along the meridional axis (y), while S3 and S4 are along the zonal axis (x). Points S5 and S6 are situated in the Bohai and Yellow Seas, respectively. The time series of depth-averaged momentum terms showed a strong correlation between variations in the pressure gradient and prevailing wind stress (Fig. 8). During periods of strong winds, the wind stress and an opposing pressure gradient were the dominant terms in the momentum budget at most of the sample locations.

For a quantitative assessment of the spatial and temporal variability in the circulation patterns, Extended Empirical Orthogonal Function (EEOF) analysis was utilized. EEOF, an extension of the traditional spatial Empirical Orthogonal Function (EOF) approach, can be used on two-dimensional vector fields such as surface winds or currents (Kaihatu et al., 1998; Thomson and Emery, 2014). The zonal (u) and meridional (v) velocity time series were combined in a complex time series $U = u + iv$. The first three modes (EEOF1, EEOF2, and EEOF3) of the currents and their corresponding principal components (PCs) are displayed in Fig. 9, with the PC amplitudes shown in Fig. 10. These three leading EEOF modes accounted for about 85 % of the total variance in the control run. Frequency spectrum analysis of the PC1 time series

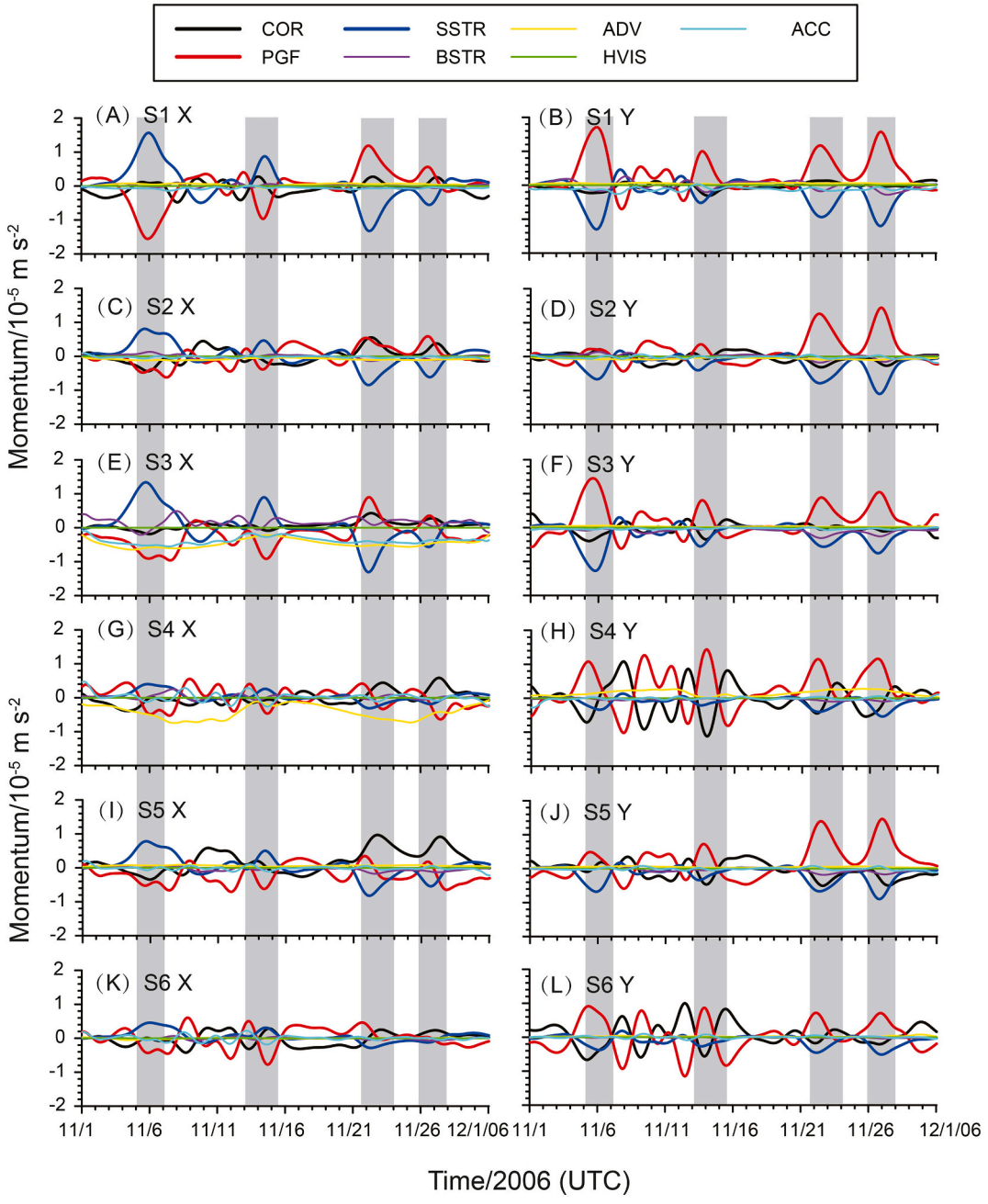

Fig. 8. Time series of depth-averaged momentum terms (units: m s^{-2}) at sites S1–S6. Sites are shown in Fig. 1 (A) as the star points.

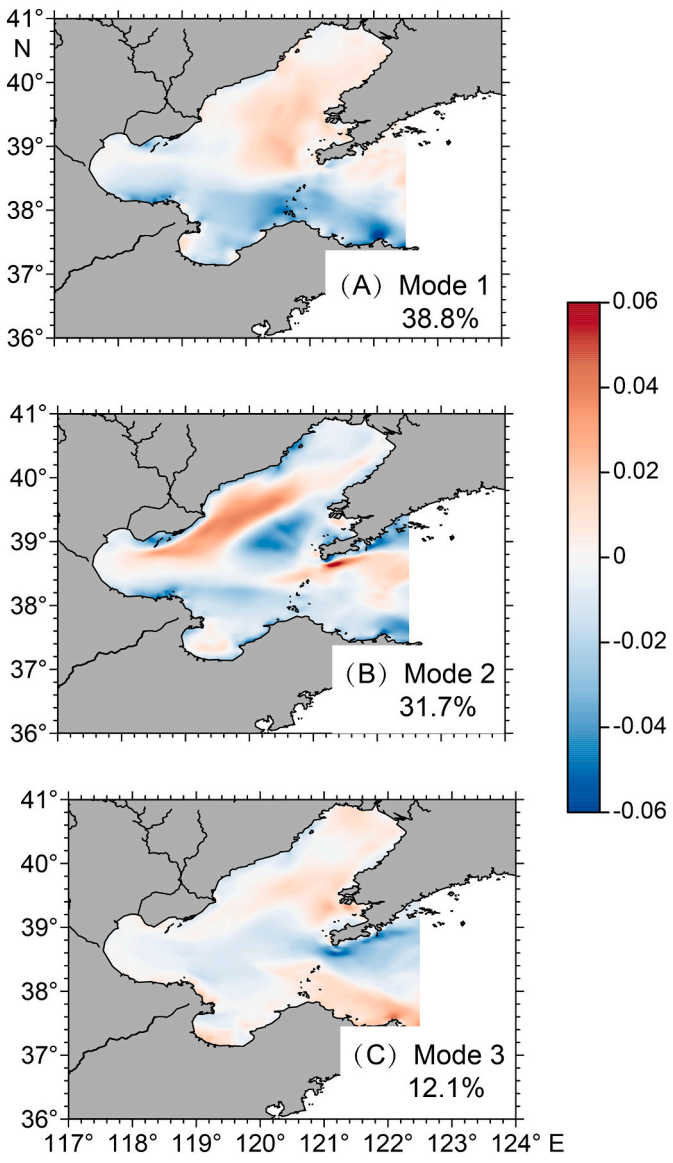

Fig. 9. Spatial patterns of the first three EEOFs of the depth-averaged currents.

corresponded with the sea surface height (SSH) difference between sites S5 and S6 (Fig. 10A), indicating that about 40 % of the synoptic current fluctuations were dependent on the pressure gradient between the Bohai and Yellow Seas. These fluctuations in the SSH difference, which control the inflow from the Yellow Sea, were most likely associated with wind-induced Coastal Trapped Waves (CTWs) in the Yellow Sea generated by storm events propagating cyclonically over the continental shelf (Brink, 1991; Ding et al., 2018; Wang et al., 2020). The time series PC2 correlated well with the east-west wind fluctuations and the SSH difference between sites S3 and S4 (Fig. 10B), with a correlation coefficient of about 0.8 between currents and the SSH difference. The variance of PC3 was consistent with fluctuations in the north-south component of the wind and the SSH difference between sites S1 and S2 (Fig. 10C) with an 18-h lag (Fig. 10C). The correlation coefficient between currents and the SSH difference was 0.7. The distance and time lag correspond with a phase speed of wave propagation of about 10 m s^{-1}, similar to the shallow water wave speed of $\sqrt{gh}$ (where $g = 9.81$ m s^{-2} is the acceleration due to gravity, and h is the water depth, Table 2). This suggests a significant influence from local wind stress and its related coastal-trapped waves, generated by local synoptic winter storms (Jacobs et al., 1998). These results indicate that about 45 % of the synoptic current fluctuations in the Bohai Sea can be attributed to local wind stress and its associated coastal-trapped waves.

To analyze the influence of the coastal-trapped waves, spectral analysis was conducted on the sea level time series at stations S1–S6. Five dominant peaks were identified in the sea level fluctuations (Fig. 11A). The most pronounced peaks, with periods of 12.4 h and 24 h, were associated with semidiurnal and diurnal tides. The amplitudes of the three smaller peaks varied from 8 to 13 cm, with periods of 60 h, 103 h, and 180 h (Fig. 11A). Wave amplitudes decreased seaward from the coast (Fig. 11B). Typical amplitudes of coastal-trapped waves are on the order of 10 cm, wavelengths are a few thousand kilometers (Mysak, 1980), and periods are between 48 h and 480 h (Clarke, 1977). Thus, these three peaks are consistent with characteristics of coastal-trapped waves. The phase velocity (ω/k) for wave periods of 60 h, 103 h, and 180 h and shallow water wave speed ($\sqrt{gh}$) were calculated at stations S1–S6. Here $\omega = 2\pi/T$ represents the radian frequency, T is the wave period, and k is the wave number, which is determined from $\omega^2 = gktanh(kh)$. The correspondence between the phase velocities based on the frequency analysis and the shallow water wave speed shows that wave propagation depends solely on the local water depth (Table 2), which is consistent with water level fluctuations from coastal trapped waves. Therefore, currents in the Bohai Sea are influenced by local winds and related coastal-trapped waves (45 %) as well as by coastal-trapped waves forced remotely from the Yellow Sea (40 %).

4.4. Sediment transport depending on wind direction

To explore the influence of wind events on sediment transport in the Bohai Sea, a spatial and temporal variations were analyzed during two specific storms (events I and IV). SSC greatly increased due to the strong winds during winter storms, with values larger than 100 mg L^{-1} along the Yellow River Delta, at the mouth of Bohai Bay, and the head of Liaodong Bay (Fig. 12). In those areas, the wave-current induced bottom shear stresses exceeded 0.2 N m^{-2}, facilitating strong sediment resuspension (Fig. 12). As a result, high values of sediment flux occurred along the south coast of the Bohai Sea (Fig. 13). As the winds diminished, a corresponding gradual reduction in wave-current induced bottom shear stress was observed, leading to a decrease in both SSC and sediment flux.

The instantaneous sediment flux was sensitive to changes in wind direction. At the onset of the northwesterly wind phase (Fig. 13A–D), sediment resuspension was enhanced by the waves and eastward sediment transport along the south coast of the Bohai Sea increased. The instantaneous sediment flux southward from Liaodong Bay to the central Bohai Sea was <10 g m^{-2} s^{-1}. Sediment was primarily transported towards the Yellow Sea through the southern part of the Bohai Strait, rather than through the northern part. As the northwesterly wind continued, the pattern of sediment transport shifted, with sediment moving into the Bohai Sea through the northern part of the Bohai Strait (Fig. 13E–H). Throughout the northwesterly wind conditions, sediment off the Yellow River Delta and along the southern coast of the Bohai Sea was resuspended and transported eastward, eventually exiting through the southern Bohai Strait (Fig. 14A).

Under northeasterly winds, the sediment transport patterns differed markedly from northwesterly wind conditions. With the northeasterly winds, sediment flux separated into three branches following the current patterns: westward into Bohai Bay, northeastward into the central Bohai Sea, and eastward along the south coast of Bohai Sea (Fig. 13I–L). As the northeasterly winds weakened, sediment continued to be transported eastward and northeastward, exiting the Bohai Sea through the southern Bohai Strait, with relatively small transport values of <10 g m^{-2} s^{-1}. Little sediment was transported into the Bohai Sea through the northern part of the Bohai Strait by a westward current (Fig. 13M–P). Consequently, the net effect of northeasterly winds was to carry sediment off the Yellow River delta westward into Bohai Bay, northeastward into the

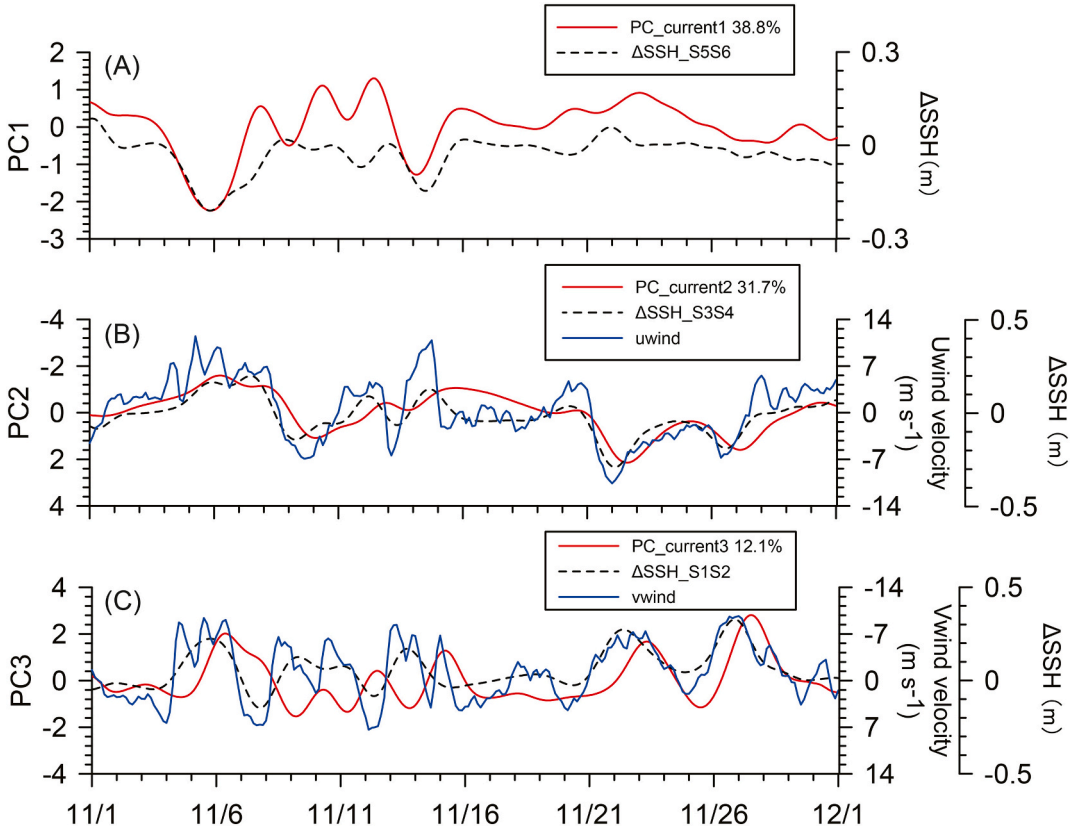

Fig. 10. Time series of the principal components (PCs) associated with the first three EEOFs, west-east wind component (uwind), north-south component (vwind), and the difference of sea surface height (SSH) between sites S1 and S2, sites S3 and S4, and sites S5 and S6 (ΔSSH_S1S2: S1–S2; ΔSSH_S3S4: S4–S3; ΔSSH_S5S6: S5–S6).

Table 2
The phase velocity (C_1, ω/k) and shallow water wave speed (C_2, $\sqrt{gh}$) at the sampling locations for wave periods (T) of 60 h, 103 h, and 180 h from the model. Units are m s^{-1}.

	S1	S2	S3	S4	S5	S6
C_1 (T = 60 h)	10.4	11.0	8.6	20.9	15.4	21.1
C_2 (T = 60 h)	10.5	11.0	8.7	21.1	15.5	21.3
C_1 (T = 103 h)	10.5	11.0	8.7	21.0	15.4	21.2
C_2 (T = 103 h)	10.5	11.0	8.7	21.1	15.5	21.3
C_1 (T = 180 h)	10.5	11.0	8.7	21.1	15.5	21.3
C_2 (T = 180 h)	10.5	11.0	8.7	21.1	15.5	21.3

central Bohai Sea, and eastward along the south coast of the Bohai Sea, eventually passing through the southern Bohai Strait (Fig. 14B).

5. Discussion

Wind statistics from the past 40 years (1979 to 2019) illustrated that strong northerly winds were interspersed with weak southerly winds in winter (October to March, Fig. 15A). Northerly winds prevailed on nearly 56 % of winter days, with a roughly equal distribution of northwesterly and northeasterly wind occurrences. However, the monthly averaged winds primarily reflected the influence of weaker northwesterly winds, with speeds <5 m s^{-1} (Fig. 15B). Models forced by monthly or seasonally averaged winds can't capture the critical forcing conditions present during storm events (e.g., strong northeasterly

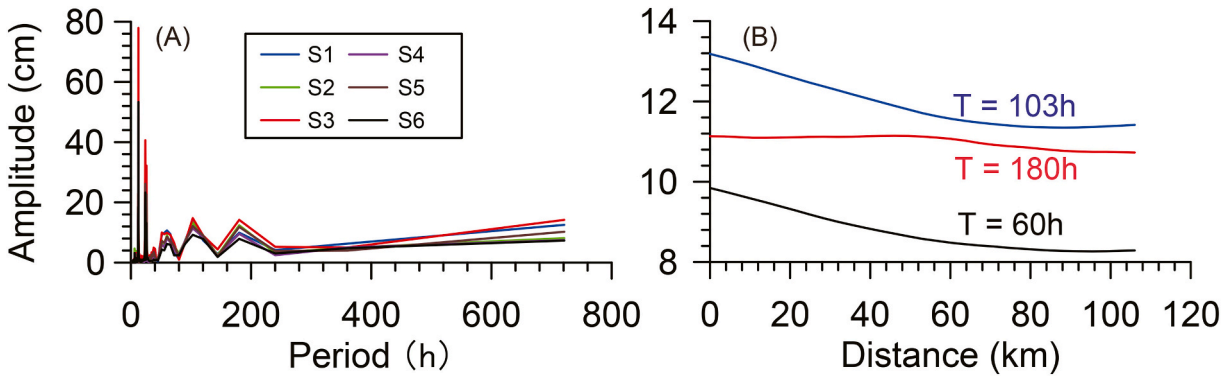

Fig. 11. Spectral analysis of sea level anomaly at stations S1–S6 (A) and amplitude of the frequencies associated with coastal-trapped waves vs. distance from the coast (MN line shown in Fig. 1(A)).

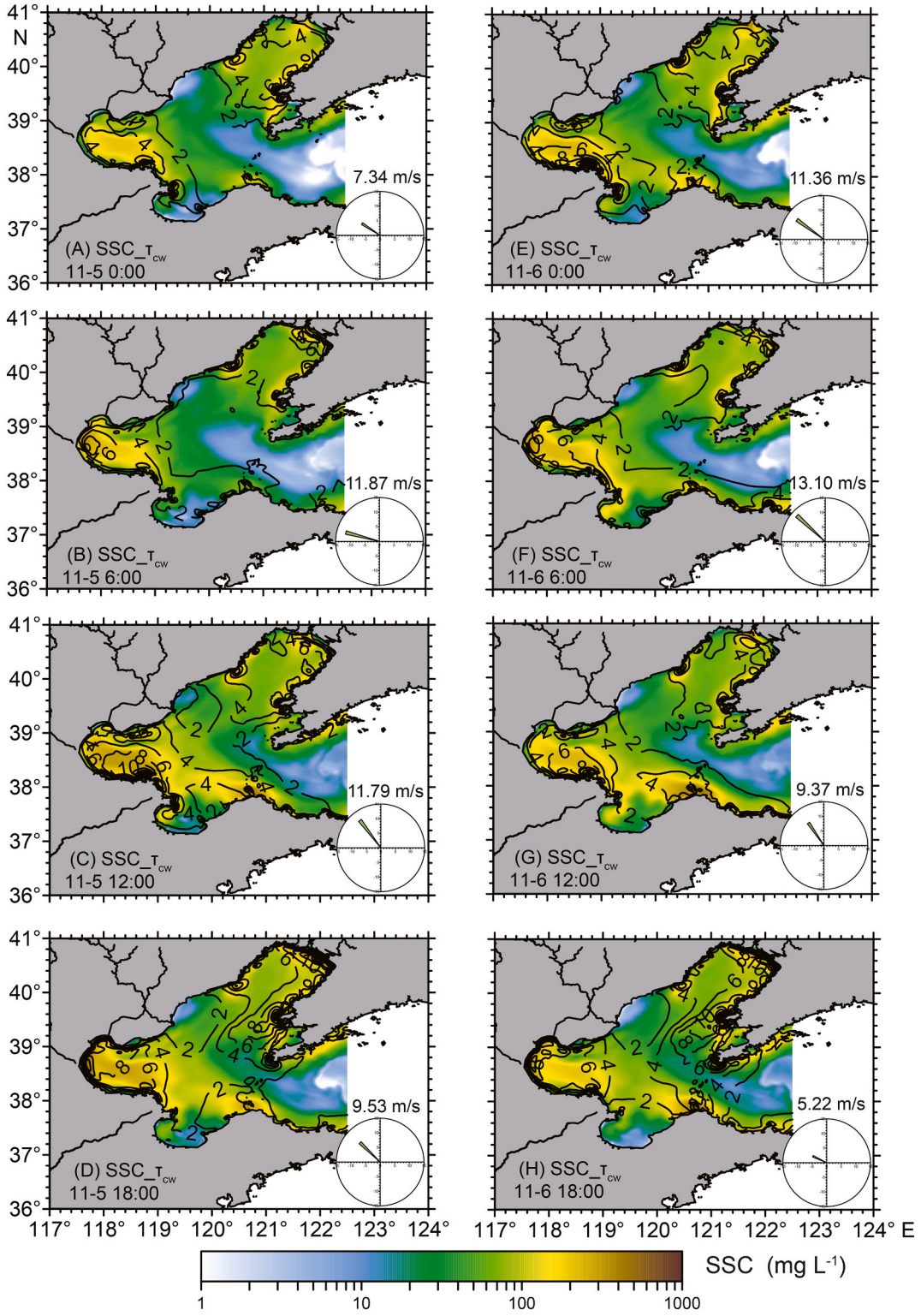

Fig. 12. Horizontal distribution of depth-averaged SSC (color, mg L^{-1}) and wave-current induced bottom shear stress (lines, $\times 10^{-1}$ N m^{-2}) from the control model results on Nov 5–6 and Nov. 26–27, with wind rose diagrams (lower right).

winds). When model forcing is based on these averages, sediment transport is primarily eastward from the Yellow River Delta into the Yellow Sea through the southern Bohai Strait (Jiang et al., 2000; Lu et al., 2011; Bian et al., 2013). Employing wind data with higher temporal resolution allows for the incorporation of current and SSC fluctuations at the scale of storm events into the overall transport.

The distribution of grain sizes in surface sediments provides insights into sediment dynamics under current environmental conditions (Gao and Collins, 1992). Based on bed surface sediment measurements by Hu (2010) and Yuan et al. (2020), the mean surface grain size in the Bohai Sea ranged from 1.84 Φ to 7.65 Φ, with an average of 5.27 Φ (Fig. 16A). Around the Yellow River Delta, a mud deposit characterized by finer

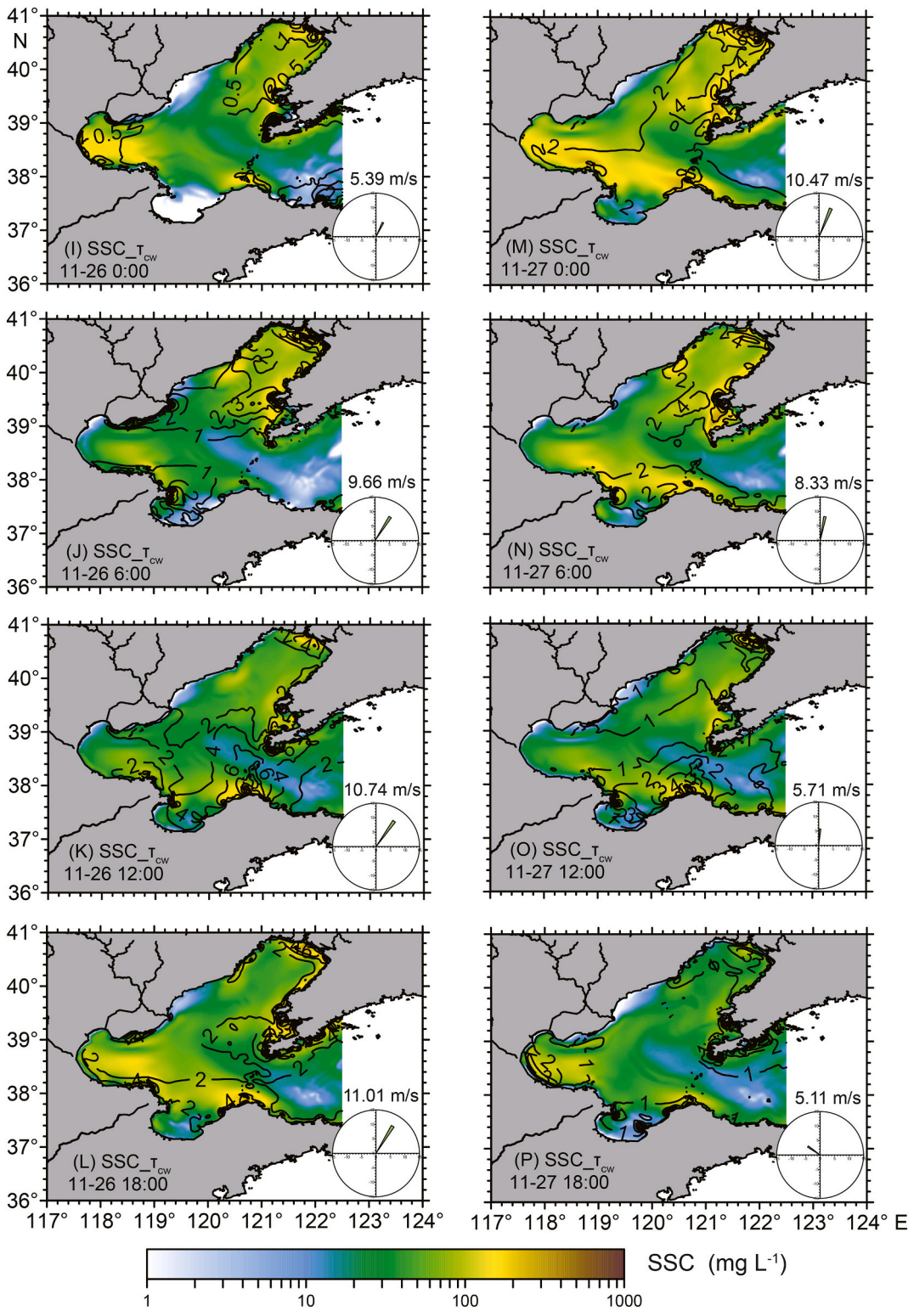

Fig. 12. (*continued*).

sediment (6–7 Φ) extended westward into Bohai Bay, northeastward into the central Bohai Basin, and eastward into Laizhou Bay, which was consistent with a previous study (Marine Geology Laboratory of Institute of Oceanology Chinese Academy of Sciences, 1985). The surface sediment in the eastern Bohai Sea was coarser and dominated by silt and sand (mean grain size <5 Φ). Near the northern Bohai Strait and adjacent areas, the surface sediment was primarily composed of coarse sediment (mean grain size of 2–3 Φ). Transport vectors, calculated from grain size parameters (mean grain size, sorting coefficient, and skewness) as proposed by Gao and Collins (1991, 1992), were used to trace the net pathways of sediment transport. By examining sediments from stations with different characteristic distances, it was determined that a maximum distance of 0.4° most accurately reflected the net surface sediment transport pattern. Results revealed two converging centers of sediment transport in the Bohai Sea: in the upper Liaodong Bay and the mud area in the central Bohai Sea (Fig. 16B). Sediment near the Yellow

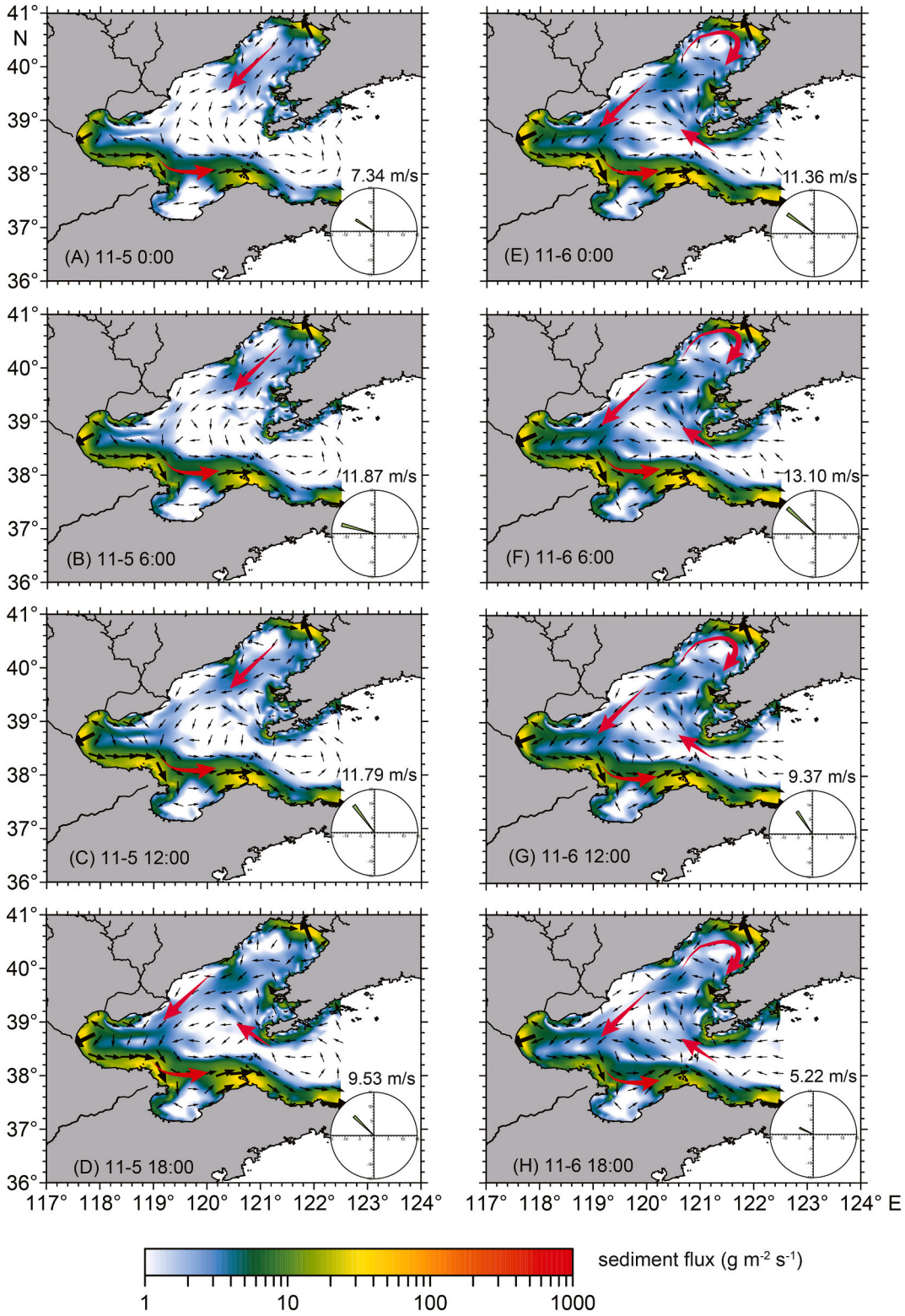

Fig. 13. Horizontal distribution of depth-averaged sediment flux from the control model results on Nov. 5–6 and Nov. 26–27, with wind rose diagrams (lower right).

River mouth was primarily transported eastward and northeastward (Fig. 16B, Yuan et al., 2020), which was consistent with the sediment transport pattern during northeasterly winds of winter storm events. Therefore, the accumulation of fine sediments northeast of the Yellow River might be linked to variability in wind strength and direction that is not represented in the mean wind conditions. This hypothesis requires further investigation and validation through additional observational evidence.

6. Conclusions

A high-resolution, coupled model of the Bohai and Yellow Seas was

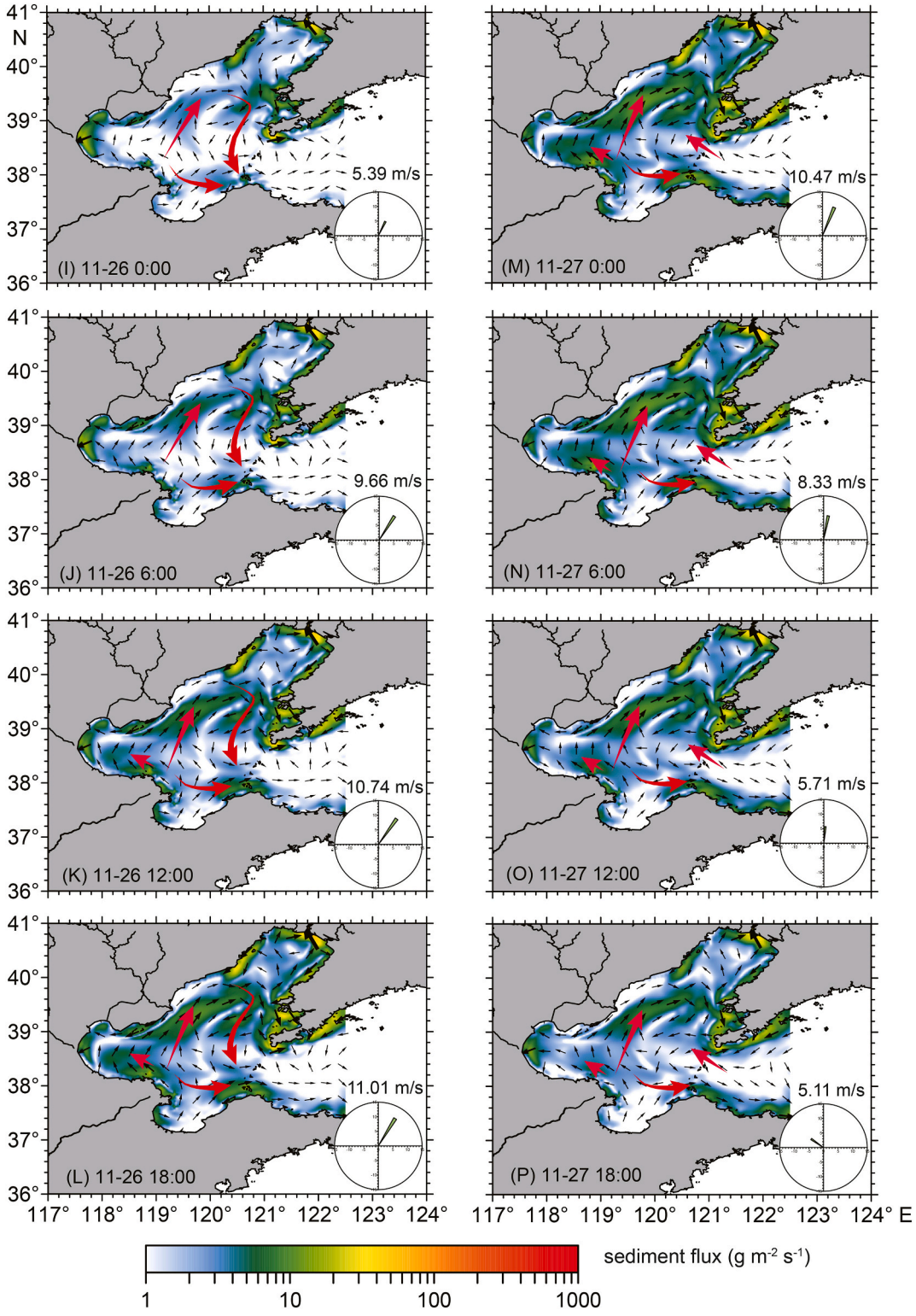

Fig. 13. (*continued*).

utilized to explore the dynamics of currents and the patterns of sediment resuspension and transport in response to episodic storms in the Bohai Sea. In winter, winds generally come from the northeast and northwest, interspersed with intermittent calmer periods. Model results driven by the fluctuating wind conditions exhibited greater complexity in the current and sediment transport patterns than those documented in previous studies, and suggest a mechanism for formation of a region of fine-grained sediment deposition near the Yellow River Delta that was previously unexplained.

Under strong northwesterly winds, currents and suspended sediment moved southward in Liaodong Bay and the central Bohai Sea before turning eastward along the south coast of the Bohai Sea and eventually being exported to the Yellow Sea through the entire Bohai Strait. With the relaxation of northwesterly winds, the currents in the northern section of the Bohai Strait shifted westward with minimal suspended sediment, whereas sediment continued to be transported eastward along

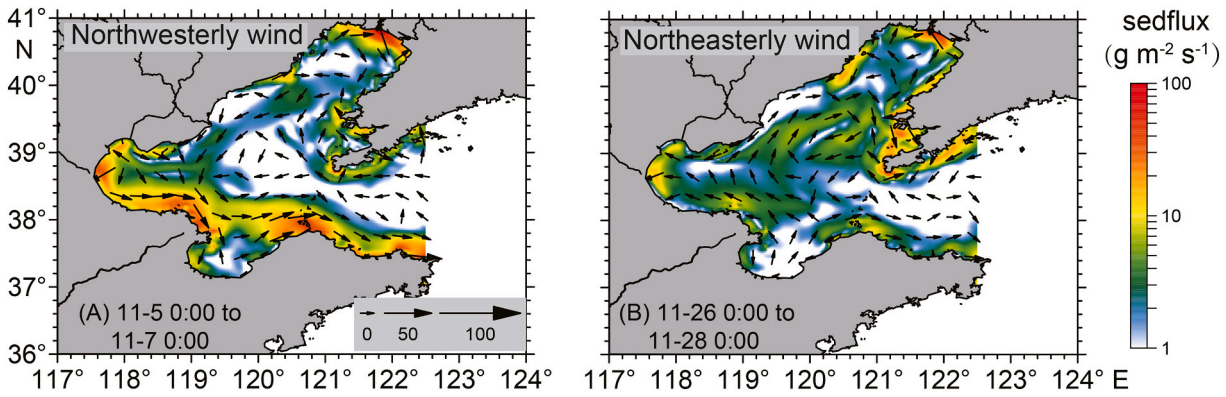

Fig. 14. Horizontal distribution of depth-averaged sediment flux in the control run over the period Nov. 5, 0:00 to Nov. 7, 0:00 (A) and Nov. 26, 0:00 to Nov. 28, 0:00 (B).

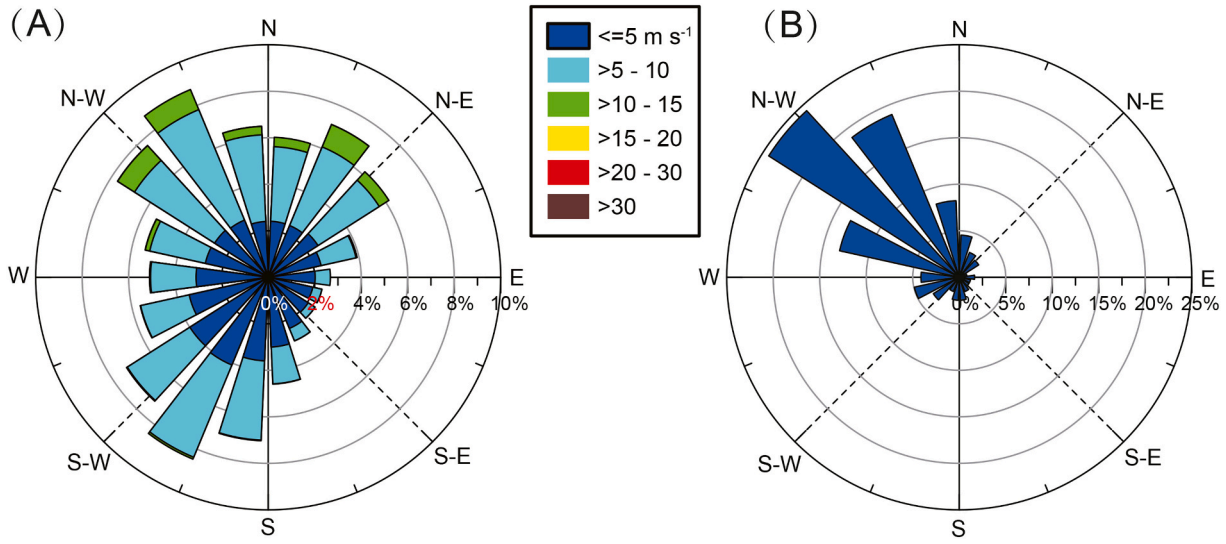

Fig. 15. Rose diagrams of 3 h-spatial averaged wind vectors (A) and monthly-spatial averaged wind vectors (B) in winter (from October to March of the next year) in the last 40 years (1979–2019). The domain for spatial average is shown in Fig. 2 (C) as the red dashed line.

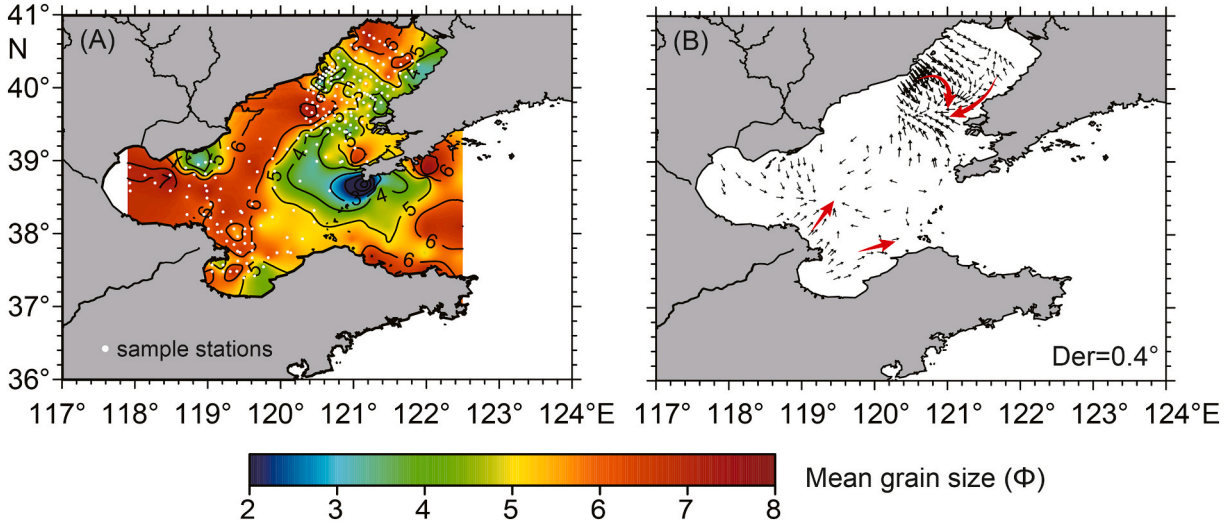

Fig. 16. Horizontal distribution of mean grain size in the surface sediments (A), net sediment transport patterns based on grain size trend analysis (B) (data source: Hu, 2010; Yuan et al., 2020). White points in (A) were sediment sample stations.

the southern coast of the Bohai Sea and through the southern Bohai Strait. Throughout the entire period of northwesterly winds, sediment resuspended from the Yellow River Delta moved eastward along the southern coast of the Bohai Sea and exited the Bohai Sea through the southern part of the Bohai Strait.

Under strong northeasterly winds, currents carrying a substantial amount of sediment branched off into three directions: northeast towards the central Bohai Basin, west towards Bohai Bay, and east towards the Yellow Sea through the Bohai Strait. With a reduction in northeasterly wind strength, currents and sediment transport shifted, with sediment moving into the Bohai Sea through the northern part of the Bohai Strait and departing through the southern part. As a result, the northeaterly winds cause sediment off the Yellow River Delta to be transported westward into Bohai Bay, northeastward towards the central Bohai Sea, and eastward along the southern coast of the Bohai Sea.

The patterns of currents and sediment transport depended both on local winds generating coastal-trapped waves in the Bohai Sea (approximately 45 %) and on remotely forced coastal-trapped waves from the Yellow Sea (40 %). These results challenge the widely held belief that sediment transport from the Yellow River in winter is dominantly eastward, and they provide a potential explanation for the formation of the fine sediment deposit observed to the northeast of the Yellow River mouth.

CRediT authorship contribution statement

Aimei Wang: Writing – review & editing, Writing – original draft, Visualization, Validation, Methodology, Funding acquisition, Formal analysis, Data curation, Conceptualization. **David K. Ralston:** Writing – review & editing, Writing – original draft, Formal analysis. **Naishuang Bi:** Writing – review & editing, Data curation. **Xiao Wu:** Writing – review & editing. **Chenghao Wang:** Writing – review & editing, Methodology. **Ping Yuan:** Writing – review & editing. **Houjie Wang:** Writing – review & editing, Supervision, Funding acquisition, Data curation, Conceptualization.

Declaration of competing interest

The authors declared that they have no conflicts of interest to this work.

Data availability

All the data that support the findings of this study are given in supporting information and are also deposited in Mendeley data set: https://doi.org/10.17632/c43phz3myw.5.

Acknowledgements

We are grateful to the editor and reviewers for their insightful suggestions on improving the science and quality of this manuscript. We would like to thank Dr. Xiangyu Li from Leibniz-Institute for Baltic Sea Research (IOW) for his constructive suggestions on the manuscript modification. This work is financially supported by the National Natural Science Foundation of China (Grant numbers of 42330407, 42106164, and 42276060), Taishan Scholar Project of Shandong Province (TS20190913).

References

Alexander, C.R., DeMaster, D.J., Nittrouer, C.A., 1991. Sediment accumulation in a modern epicontinental-shelf setting: the Yellow Sea. Mar. Geol. 98 (1), 51–72. https://doi.org/10.1016/0025-3227(91)90035-3.

Bi, N., Yang, Z., Wang, H., Hu, B., Ji, Y., 2010. Sediment dispersion pattern off the present Huanghe (Yellow River) subdelta and its dynamic mechanism during normal river discharge period. Estuar. Coast. Shelf Sci. 86 (3), 352–362. https://doi.org/10.1016/j.ecss.2009.06.005.

Bi, N., Yang, Z., Wang, H., Fan, D., Sun, X., Lei, K., 2011. Seasonal variation of suspended-sediment transport through the southern Bohai Strait. Estuar. Coast. Shelf Sci. 93 (3), 239–247. https://doi.org/10.1016/j.ecss.2011.03.007.

Bian, C., Jiang, W., Greatbatch, R.J., 2013. An exploratory model study of sediment transport sources and deposits in the Bohai Sea, Yellow Sea, and East China Sea. J. Geophys. Res. Oceans. 118, 5908–5923. https://doi.org/10.1002/2013JC009116.

Booij, N., Ris, R.C., Holthuijsen, L.H., 1999. A third-generation wave model for coastal regions: 1. Model description and validation. J. Geophys. Res. Oceans. 104 (C4), 7649–7666. https://doi.org/10.1029/98JC02622.

Brand, A., Lacy, J.R., Hsu, K., Hoover, D., Gladding, S., Stacey, M.T., 2010. Wind-enhanced resuspension in the shallow waters of South San Francisco Bay: Mechanisms and potential implications for cohesive sediment transport. J. Geophys. Res. Oceans. 115, C11024. https://doi.org/10.1029/2010JC006172.

Brink, K.H., 1991. Coastal-trapped waves and wind-driven currents over the continental shelf. Annu. Rev. Fluid Mech. 23, 389–412. https://doi.org/10.1146/annurev.fl.23.010191.002133.

Cheng, P., Gao, S., Bokuniewicz, H., 2004. Net sediment transport patterns over the Bohai Strait based on grain size trend analysis. Estuar. Coast. Shelf Sci. 60 (2), 203–212. https://doi.org/10.1016/j.ecss.2003.12.009.

Cheng, X., Zhu, J., Chen, S., 2021. Extensions of the river plume under various Yellow River courses into the Bohai Sea at different times. Estuar. Coast. Shelf Sci. 249, 107092 https://doi.org/10.1016/j.ecss.2020.107092.

Clarke, A.J., 1977. Observational and numerical evidence for wind-forced coastal trapped long waves. J. Phys. Oceanogr. 7, 231–247. https://doi.org/10.1175/1520-0485(1977)007<0231:OANEFW>2.0.CO;2.

Ding, Y., Bao, X., Yao, Z., Song, D., Song, J., Gao, J., Li, J., 2018. Effect of coastal-trapped waves on the synoptic variations of the Yellow Sea warm current during winter. Cont. Shelf Res. 167, 14–31. https://doi.org/10.1016/j.csr.2018.08.003.

Ding, Y., Bao, X., Yao, Z., Bi, C., Wan, K., Bao, M., Jiang, Z., Song, J., Gao, J., 2019. Observational and model studies of synoptic current fluctuations in the Bohai Strait on the Chinese continental shelf. Ocean Dyn. 69 (3), 323–351. https://doi.org/10.1007/s10236-019-01247-5.

Dong, L.X., Guan, W.B., Chen, Q., Li, X.H., Liu, X.H., Zeng, X.M., 2011. Sediment transport in the Yellow Sea and East China Sea. Estuar. Coast. Shelf Sci. 93 (3), 248–258. https://doi.org/10.1016/j.ecss.2011.04.003.

Duan, H., Xu, J., Wu, X., Wang, H., Liu, Z., Wang, C., 2020. Periodic oscillation of sediment transport influenced by winter synoptic events, Bohai Strait, China. Water 12 (4), 986. https://doi.org/10.3390/w12040986.

Enriquez, A., 2004. An Investigation of Surface Current Patterns Related to Upwelling in Monterey Bay Using High Frequency Radar. Naval Postgraduate School, Monterey, CA.

Fan, R., Wei, H., Zhao, L., Zhao, W., Jiang, C., Nie, H., 2019. Identify the impacts of waves and tides to coastal suspended sediment concentration based on high-frequency acoustic observations. Mar. Geol. 408, 154–164. https://doi.org/10.1016/j.margeo.2018.12.005.

Fang, Y., Fang, G., Zhang, Q., 2000. Numerical simulation and dynamic study of the wintertime circulation of the Bohai Sea. Chin. J. Oceanol. Limnol. 18 (1), 1–9. https://doi.org/10.1007/BF02842535.

Gao, S., Collins, M., 1991. A critique of the 'McLaren method' for defining sediment transport paths – discussion. J. Sediment. Petrol. 61 (1), 143–146. https://doi.org/10.1306/D42676A9-2B26-11D7-8648000102C1865D.

Gao, S., Collins, M., 1992. Net sediment transport patterns inferred from grain-size trends, based upon definition of 'transport vectors'. Sediment. Geol. 81 (1–2), 47–60. https://doi.org/10.1016/0037-0738(92)90055-V.

Grant, W.D., Madsen, O.S., 1979. Combined wave and current interaction with a rough bottom. J. Geophys. Res. Oceans. 84 (C4), 1797–1808. https://doi.org/10.1029/JC084iC04p01797.

Guan, B., 1994. Patterns and structures of the currents in Bohai, Huanghai and East China Seas. In: Oceanology of China Seas. Springer, Dordrecht, pp. 17–26. https://doi.org/10.1007/978-94-011-0862-1_3.

Hsu, P.C., 2022. Surface Current Variations and Hydrological Characteristics of the Penghu Channel in the Southeastern Taiwan Strait. Remote Sens. 14 (8), 1816. https://doi.org/10.3390/rs14081816.

Hu, L.M., 2010. Sources and Sink of Sedimentary Organic Matter in the River-Dominated Continental Shelves: A Case Study in the Bohai and Yellow Seas. Ocean University of China, PhD, pp. 1–190.

Hu, Z., Wang, D.P., He, X., Li, M., Wei, J., Pan, D., Bai, Y., 2017. Episodic surface intrusions in the Yellow Sea during relaxation of northerly winds. J. Geophys. Res. Oceans. 122, 6533–6546. https://doi.org/10.1002/2017JC012830.

Huang, D., Su, J., Backhaus, J.O., 1999. Modelling the seasonal thermal stratification and baroclinic circulation in the Bohai Sea. Cont. Shelf Res. 19 (11), 1485–1505. https://doi.org/10.1016/S0278-4343(99)00026-6.

Jacob, R., Larson, J., Ong, E., 2005. M × N communication and parallel interpolation in community climate system model version 3 using the model coupling toolkit. Int. J. High Perform. Comp. Appl. 19 (3), 293–307. https://doi.org/10.1177/1094342005056116.

Jacobs, G.A., Preller, R.H., Riedlinger, S.K., Teague, W.J., 1998. Coastal wave generation in the Bohai Bay and propagation along the Chinese coast. Geophys. Res. Lett. 25 (6), 777–780. https://doi.org/10.1029/97GL03636.

Jiang, W., Pohlmann, T., Sundermann, J., Feng, S., Sundermann, J., Feng, S., 2000. A modelling study of SPM transport in the Bohai Sea. J. Mar. Syst. 24 (3–4), 175–200. https://doi.org/10.1016/S0924-7963(99)00071-8.

Kaihatu, J.M., Handler, R.A., Marmorino, G.O., Shay, L.K., 1998. Empirical orthogonal function analysis of ocean surface currents using complex and real-vector methods. J. Atmos. Ocean. Technol. 15 (4), 927–941. https://doi.org/10.1175/1520-0426(1998)015<0927:EOFAOO>2.0.CO;2.

Larson, J., Jacob, R., Ong, E., 2005. The model coupling toolkit: a new Fortran90 toolkit for building multiphysics parallel coupled models. Int. J. High Perform. Comp. Appl. 19 (3), 277–292. https://doi.org/10.1177/1094342005056115.

Li, M., Wu, Y., Prescott, R.H., Tang, C.C.L., Han, G., 2015. A modeling study of the impact of major storms on waves, surface and near-bed currents on the Grand Banks of Newfoundland. J. Geophys. Res. Oceans. 120, 5358–5386. https://doi.org/10.1002/2015JC010755.

Lin, X., Yang, J., 2011. An asymmetric upwind flow, Yellow Sea warm current: 2. Arrested topographic waves in response to the northwesterly wind. J. Geophys. Res. Oceans. 116, C04027. https://doi.org/10.1029/2010JC006514.

Liu, J., Milliman, J., Gao, S., Cheng, P., 2004. Holocene development of the Yellow River's subaqueous delta, North Yellow Sea. Mar. Geol. 209 (1–4), 45–67. https://doi.org/10.1016/j.margeo.2004.06.009.

Liu, X., Qiao, L., Zhong, Y., Qan, X., Xue, W., Liu, P., 2020. Pathways of suspended sediments transported from the Yellow river mouth to the Bohai Sea and Yellow Sea. Estuar. Coast. Shelf Sci. 236, 106639 https://doi.org/10.1016/j.ecss.2020.106639.

Liu, Z., Gan, J., 2014. Modeling study of variable upwelling circulation in the East China Sea: response to a coastal promontory. J. Phys. Oceanogr. 44, 1078–1094. https://doi.org/10.1175/JPO-D-13-0170.1.

Lu, J., Qiao, F.L., Wang, X.H., Wang, Y.G., Teng, Y., Xia, C.S., 2011. A numerical study of transport dynamics and seasonal variability of the Yellow River sediment in the Bohai and Yellow Seas. Estuar. Coast. Shelf Sci. 95 (1), 39–51. https://doi.org/10.1016/j.ecss.2011.08.001.

Madsen, O.S., 1994. Spectral wave–current bottom boundary layer flows. In: Coastal engineering 1994. In: In: Proceedings of the 24th International Conference on Coastal Engineering Research Council. Kobe, Japan, pp. 384–398. https://doi.org/10.1061/9780784400890.030.

Marine Geology Laboratory of Institute of Oceanology Chinese Academy of Sciences, 1985. The Bohai Sea Geology. Science Press, Beijing, pp. 1–232 (in Chinese).

Martin, J., Zhang, J., Shi, M., Zhou, Q., 1993. Actual flux of the Huanghe(Yellow River) sediment to the western Pacific Ocean. Neth. J. Sea Res. 31 (3), 243–254. https://doi.org/10.1016/0077-7579(93)90025-N.

Miles, T., Glebb, S.M., Schofiled, O., 2013. Temporal and spatial variability in fall storm induced sediment resuspension on the mid-Atlantic Bight. Cont. Shelf Res. 63, S36–S49. https://doi.org/10.1016/j.csr.2012.08.006.

Milliman, J.D., Meade, R.H., 1983. World-wide delivery of river sediment to the oceans. J. Geol. 91 (1), 1–21. https://doi.org/10.1086/628741.

Mysak, L.A., 1980. Recent advances in shelf wave dynamics. Rev. Geophys. 18 (1), 211–241. https://doi.org/10.1029/RG018i001p00211.

Paduan, J.D., Cook, M.S., Tapia, V.M., 2018. Patterns of upwelling and relaxation around Monterey bay based on long-term observations of surface currents from high frequency radar. Deep-Sea Res. II 151, 129–136. https://doi.org/10.1016/j.dsr2.2016.10.007.

Qiao, S.Q., Shi, X.F., Wang, G.Q., Yang, G., Hu, N.J., Liu, S.F., Liu, Y.G., Zhu, A.M., Li, C. X., 2010. Discussion on grain-size characteristics of seafloor sediment and transport pattern in the Bohai Sea. Acta Oceanol. Sin. 32 (4), 139–147 (in Chinese with English Abstract).

Qin, Y., Li, F., Zheng, T., Xu, S., 1986. A study on total suspended matter in winter in the south Yellow Sea. Mar. Sci. 10 (6), 1–7 (In Chinese with English abstract).

Qin, Y., Li, F., Xu, S., Milliman, J., Limeburner, R., 1989. Suspended matter in the south Yellow Sea. Oceanol. Limnol. Sin. 20 (2), 101–112 (In Chinese with English abstract).

Qin, Y.S., Li, F., 1983. Study of influence of sediment loads discharged from the Huanghe River on sedimentation in the Bohai Sea and the Huanghai Sea. In: Proceedings of the International Symposium on Sedimentation on the Continental Shelf with Special Reference to the East China Sea. China Ocean Press, Beijing, 83–92 (In Chinese).

Qu, L., Lin, X., Hetland, R.D., Guo, J., 2018. The asymmetric continental shelf wave in response to the synoptic wind burst in a semienclosed double-shelf basin. J. Geophys. Res. Oceans. 123, 131–148. https://doi.org/10.1002/2017JC013025.

Sanford, L.P., 1994. Wave-forced resuspension of upper Chesapeake Bay muds. Estuaries 17 (1), 148–165. https://doi.org/10.2307/1352564.

Schoellhamer, D.H., 1995. Sediment resuspension mechanisms in old Tampa bay, Florida. Estuar. Coast. Shelf Sci. 40 (6), 603–620. https://doi.org/10.1006/ecss.1995.0041.

Shchepetkin, A.F., Mcwilliams, J.C., 2005. The regional oceanic modeling system (ROMS): a split-explicit, free-surface, topography-following-coordinate oceanic model. Ocean Model 9 (4), 347–404. https://doi.org/10.1016/j.ocemod.2004.08.002.

Shen, J., Zhang, J., Qiu, Y., Li, L., Zhang, S., Pan, A., Huang, J., Guo, X., Jing, C., 2019. Winter counter-wind current in western Taiwan Strait: characteristics and mechanisms. Cont. Shelf Res. 172, 1–11. https://doi.org/10.1016/j.csr.2018.11.005.

Shi, J.Z., Gu, W.J., Wang, D.Z., 2008. Wind wave-forced fine sediment erosion during the slack water periods in Hangzhou Bay, China. Environ. Geol. 55, 629–638. https://doi.org/10.1007/s00254-007-1013-2.

Sun, X.W., Xi, P.G., 1988. The results of the 3D nonlinear tidal boundary problem and its analysis. J. Shandong Coll. Oceanogr. 18, 51–52 (in Chinese with English abstract).

Teague, W.J., Jacobs, G.A., 2000. Current observations on the development of the Yellow Sea warm current. J. Geophys. Res. Oceans. 105 (C2), 3401–3411. https://doi.org/10.1029/1999JC900301.

Thomson, R.E., Emery, W.J., 2014. Data Analysis Methods in Physical Oceanography, third ed. Elsevier, Waltham, MA.

Wan, X., Ma, Q., Ma, W., 2015. The effect of high frequency strong winds on winter circulation and water exchange in the Bohai Sea by ROMS. Period. Ocean Univ. 45 (4), 1–8 (in Chinese with English abstract).

Wang, A., Ralston, D.K., Bi, N., Cheng, Z., Wu, X., Wang, H., 2019. Seasonal variation in sediment transport and deposition on a muddy clinoform in the Yellow Sea. Cont. Shelf Res. 179, 37–51. https://doi.org/10.1016/j.csr.2019.04.009.

Wang, A., Wu, X., Bi, N., Ralston, D.K., Wang, C., Wang, H., 2022. Combined effects of waves and tides on bottom sediment resuspension in the southern Yellow Sea. Mar. Geol. 452, 106892 https://doi.org/10.1016/j.margeo.2022.106892.

Wang, C., Liu, Z., Harris, C.K., Wu, X., Wang, H., Bian, C., Bi, N., Duan, H., Xu, J., 2020. The impact of winter storms on sediment transport through a narrow strait, Bohai, China. J. Geophys. Res. Oceans. 125 (6) https://doi.org/10.1029/2020JC016069 e2020JC016069.

Wang, H., Yang, Z., Saito, Y., Liu, J.P., Sun, X., Wang, Y., 2007. Stepwise decreases of the Huanghe (Yellow River) sediment load (1950–2005): impacts of climate change and human activities. Glob. Planet. Chang. 57 (3–4), 331–354. https://doi.org/10.1016/j.gloplacha.2007.01.003.

Wang, H., Wang, A., Bi, N., Zeng, X., Xiao, H., 2014. Seasonal distribution of suspended sediment in the Bohai Sea, China. Cont. Shelf Res. 90, 17–32. https://doi.org/10.1016/j.csr.2014.03.006.

Wang, L., Pawlowicz, R., Wu, X., Yue, X., 2021. Wintertime variability of currents in the southwestern Taiwan Strait. J. Geophys. Res. Oceans. 126 https://doi.org/10.1029/2020JC016586 e2020JC016586.

Wang, Q., XG, Takeoka, H., 2008. Seasonal variations of the Yellow River plume in the Bohai Sea: a model study. J. Geophys. Res. Oceans. 113, C08046. https://doi.org/10.1029/2007JC004555.

Warner, J.C., Sherwood, C.R., Signell, R.P., Harris, C.K., Arango, H.G., 2008. Development of a three-dimensional, regional, coupled wave, current, and sediment transport model. Comput. Geosci. 34 (10), 1284–1306. https://doi.org/10.1016/j.cageo.2008.02.012.

Warner, J.C., Armstrong, B., He, R., Zambon, J.B., 2010. Development of a coupled Ocean–Atmosphere–Wave–Sediment Transport (COAWST) Modeling System. Ocean Model 35 (3), 230–244. https://doi.org/10.1016/j.ocemod.2010.07.010.

Wu, H., Gu, J., Zhu, P., 2018. Winter counter-wind transport in the inner southwestern Yellow Sea. J. Geophys. Res. Oceans. 123, 411–436. https://doi.org/10.1002/2017JC013403.

Wu, X., Wu, H., Wang, H., Bi, N., Duan, H., Wang, C., Bian, C., Xu, J., 2019a. Novel, repeated surveys reveal new insights on sediment flux through a Narrow Strait, Bohai, China. J. Geophys. Res. Oceans. 124, 6927–6941. https://doi.org/10.1029/2019JC015293.

Wu, X., Xu, J., Wu, H., Bi, N., Bian, C., Li, P., Wang, A., Duan, H., Wang, H., 2019b. Synoptic variations of residual currents in the Huanghe (Yellow River)-derived distal mud patch off the Shandong Peninsula: Implications for long-term sediment transport. Mar. Geol. 417, 106014 https://doi.org/10.1016/j.margeo.2019.106014.

Yang, Z., Liu, J., 2007. A unique Yellow River-derived distal subaqueous delta in the Yellow Sea. Mar. Geol. 240 (1–4), 169–176. https://doi.org/10.1016/j.margeo.2007.02.008.

Yang, Z., Ji, Y., Bi, N., Lei, K., Wang, H., 2011. Sediment transport off the Huanghe (Yellow River) delta and in the adjacent Bohai Sea in winter and seasonal comparison. Estuar. Coast. Shelf Sci. 93 (3), 173–181. https://doi.org/10.1016/j.ecss.2010.06.005.

Yu, F., Zhang, Z., Diao, X., Guo, J., 2010. Observational evidence of the Yellow Sea warm current. Chin. J. Oceanol. Limnol. 28, 677–683. https://doi.org/10.1007/s00343-010-0006-2.

Yuan, D., Hsueh, Y., 2010. Dynamics of the cross-shelf circulation in the Yellow and East China Seas in winter. Deep-Sea Res. II Top. Stud. Oceanogr. 57 (19–20), 1745–1761. https://doi.org/10.1016/j.dsr2.2010.04.002.

Yuan, D., Zhu, J., Li, C., Hu, D., 2008. Cross-shelf circulation in the Yellow and East China Seas indicated by MODIS satellite observations. J. Mar. Syst. 70 (1–2), 134–149. https://doi.org/10.1016/j.jmarsys.2007.04.002.

Yuan, P., Wang, H., Xiao, W., Bi, N., 2020. Grain-size distribution of surface sediments in the Bohai Sea and the Northern Yellow Sea: sediment supply and hydrodynamics. J. Ocean Univ. China 19 (3), 589–600. https://doi.org/10.1007/s11802-020-4221-y.

Zeng, X., He, R., Xue, Z., Wang, H., Wang, Y., Yao, Z., Guan, W., Warrillow, J., 2015. River-derived sediment suspension and transport in the Bohai, Yellow, and East China Seas: a preliminary modeling study. Cont. Shelf Res. 111, 112–125. https://doi.org/10.1016/j.csr.2015.08.015.

Zhou, F., Huang, D., Xue, H., Xuan, J., Yan, T., Ni, X., Zeng, D., Li, J., 2017. Circulations associated with cold pools in the Bohai Sea on the Chinese continental shelf. Cont. Shelf Res. 137, 25–38. https://doi.org/10.1016/j.csr.2017.02.005.